Dalton Transactions

Accepted Manuscript

ROYAL SOCIETY OF CHEMISTRY

www.rsc.org/dalton

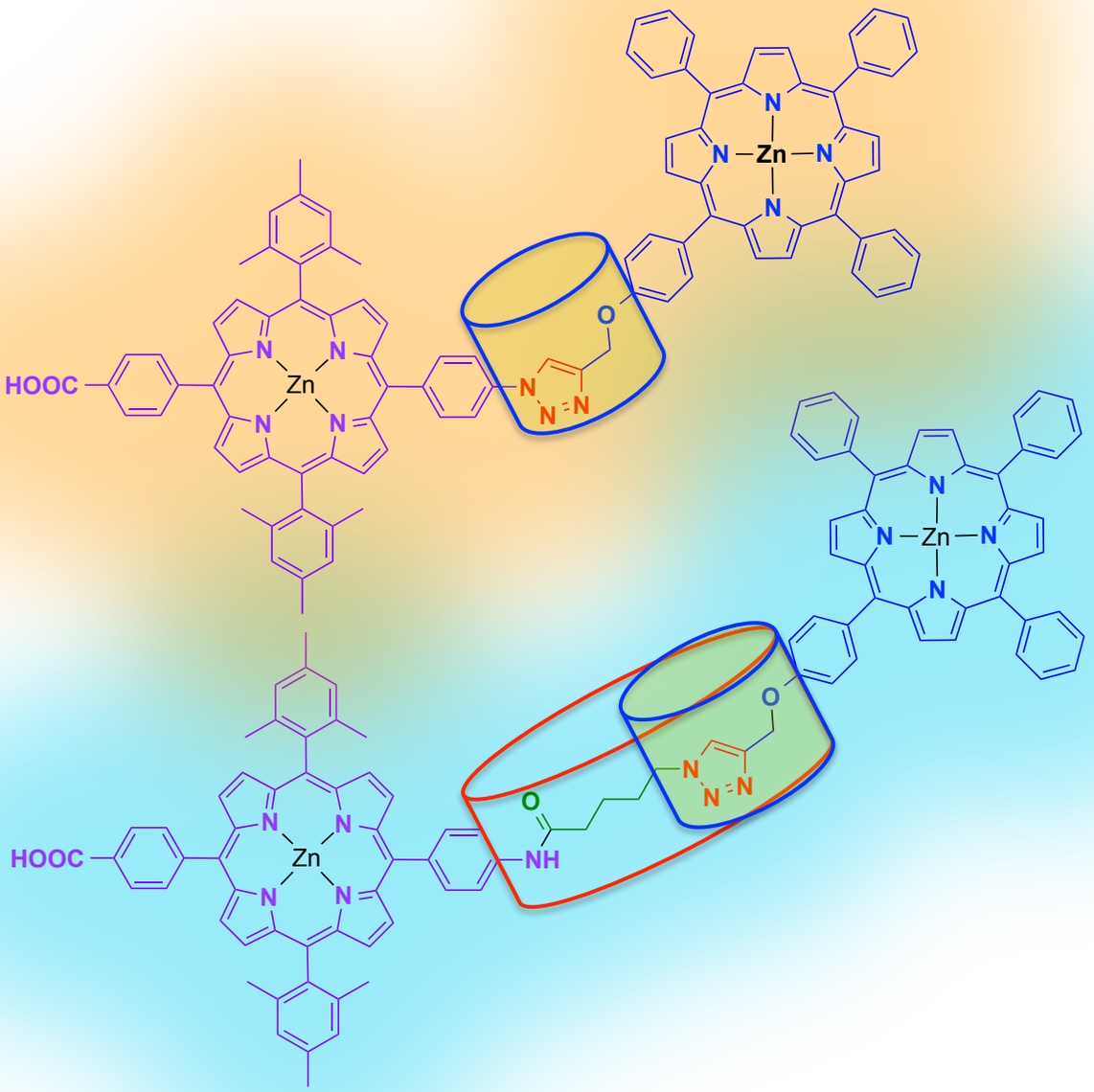

"Click-chemistry" approach for the synthesis of porphyrin dyads as sensitizers for dye-sensitized solar cells

Vasilis Nikolaou,[†] *Panagiotis A. Angaridis,*[§] *Georgios Charalambidis,*[†] *Ganesh D. Sharma,*[*,‡] *and Athanassios G. Coutsolelos*[*,†]

[†] Department of Chemistry, University of Crete, Laboratory of Bioinorganic Chemistry, Voutes Campus, P.O. Box 2208, 71003, Heraklion, Crete, Greece

[§] Department of Chemistry, Aristotle University of Thessaloniki, Thessaloniki, 54124, Greece

[‡] R&D Center for Engineering and Science, JEC group of Colleges, Jaipur Engineering College campus, Kukas, Jaipur (Raj.) 303101, India

keywords: porphyrin dyads, click reactions, dye-sensitized solar cells

ABSTRACT: Two novel porphyrin dyads (**9** and **11**) consisted of two zinc-metallated porphyrin units, covalently linked at their peripheries though 1,2,3-triazole containing bridges and functionalized by a terminal carboxylic acid group, have been synthesized via "click" reactions, which are Cu-catalyzed Huisgen 1,3-dipolar cycloadditions between azide- and acetylene-containing porphyrins. Photophysical and electrochemical measurements, together with DFT calculations, showed that the two dyads possess suitable frontier orbital energy levels for use as sensitizers in DSSCs. The **9** and **11** based solar cells were fabricated resulting in power conversion efficiencies (PCEs) of 3.82 and 5.16%, respectively. As shown by photovoltaic measurements (*J-V* curves) and incident photon to current conversion efficiency (IPCE) spectra of the two solar cells, the higher PCE value of the latter is attributed to its enhanced photovoltaic parameters, and particularly its enhanced short circuit current (J_{sc}). This is related to the stronger absorption profile of the sensitizing dyad **11** (the dyad with the shorter triazole containing bridge) and the higher dye loading of the corresponding solar cell. Furthermore, electrochemical impedance spectra (EIS) demonstrated that the **11** based solar cell exhibits longer electron lifetime (τ_e) and more effective suppression of the recombination between injected electrons and electrolyte.

INTRODUCTION

Over the last decade, dye-sensitized solar cells (DSSCs) have attracted significant interest as potential alternatives to the amorphous silicon-based solar cells, due to their low production cost, simple fabrication, and controllable optical properties. [1-5] Such devices consist of a working electrode (anode) composed of a dye-sensitized, wide band-gap metal oxide semiconductor, usually TiO_2 or ZnO, deposited on a transparent conducting oxide glass substrate, a counter electrode (cathode) composed of a Pt-coated conducting oxide glass substrate, and an electrolyte containing a redox couple, such as I^-/I_3^-. The sensitizing dye is a key element in achieving high power conversion efficiencies (PCEs), as it is responsible for photon harvesting, excitation of electrons, and injection of excited electrons into the metal oxide semiconductor conduction band (CB). Ruthenium-polypyridyl complexes have been proved to be very efficient as sensitizers, achieving high photovoltaic efficiencies above 11%, but high-cost and scarcity of ruthenium, as well as related environmental issues, prevent their affordable commercial application.[6, 7] Therefore, in recent years, extensive efforts have been directed towards the exploration of new, low-cost and efficient metal-free organic sensitizers.[8-18]

Porphyrins appear to be a very promising class of sensitizers of this type, owing to their enhanced light harvesting potential (they display an intense absorption in the 400-450 nm region, Soret band, and moderate absorptions in the 550-700 nm region, Q-bands), as well as their simple, low-cost and environmental friendly synthetic procedures.[19-22] Moreover, their physical, optical, and electronic properties can be appropriately modulated by suitable functionalization of their *meso* and *β* positions, following established molecular design procedures.[23-36] In particular, porphyrins with a donor-π-acceptor (D-π-A) molecular architecture ("push-pull") have attracted much attention,[37-41] resulting in PCE values as high as 13%.[42, 43]

In an effort to further improve the performance of porphyrin based solar cells, multi-porphyrin arrays consisted of covalently linked porphyrin macrocycles, linked either through suitable π-conjugated groups or directly, have been investigated as sensitizers. Due to extended conjugation, the photophysical properties of such systems appear to be enhanced and their characteristic absorptions and emissions are shifted to longer wavelengths, compared to single porphyrins. For example, ethynyl-bridged porphyrins through their *meso* positions display strong electronic coupling between porphyrin macrocycles resulting in splitting of their Soret band and broadening of their Q bands.[44] Furthermore, directly linked porphyrins[45] and fused porphyrins arrays[46-48] exhibit broad absorptions, covering the visible and near IR regions of solar spectrum. Solar cells based on such dyes allow the exploitation of lower energy photons and have the potential to lead to enhanced light harvesting and overall solar cell efficiencies. Corroborating the above, a DSSC based on an ethynyl-bridged carbazole-porphyrin-porphyrin triad showed efficient light to current conversion throughout the visible to near IR regions achieving a PCE value of 5.21 %.[49] In addition, we recently reported the use of porphyrin dyads and triads as sensitizers in DSSCs achieving PCE values in the range 4-6 %.[50-52]

Among the various synthetic strategies that have been applied towards the synthesis of multi-porphyrin assemblies, transition metal catalytic reactions play a very important role. In particular, Pd-based cross-coupling reactions, through the formation of C-C and C-N bonds, have been proved to be a powerful tool for the construction of elaborate architectures, though simple, versatile, and cost- and time-efficient routes. Alkynyl- and alkenyl-bridged systems can be synthesized via Sonogashira[53] and Heck reactions[54, 55] respectively. Furthermore, still reactions based on organotin compounds can be utilized for the synthesis of alkenyl-, alkynyl- and aryl-bridged assemblies,[56] while Suzuki reactions based on organoboron

compounds are used for linking aromatic groups.[57] Finally, connection though C-N bonds can be achieved via Bachwald-Hartwig reactions.[58, 59]

Another type of metal catalyzed reactions that has recently received great attention for the construction of multi-chromophore arrays is "click" reactions.[60] Click chemistry is a powerful method to synthesize new compounds in a reliable and selective way by linking two chemical moieties together, which has found many applications in chemical synthesis, drug discovery, chemical biology, and proteomic applications.[61] On the other hand, in porphyrin chemistry it is highly desirable to have available a simple, efficient and versatile synthetic strategy for functionalizing porphyrin units, in order to be used in various areas of interest. Towards this direction, the utilization of click reaction between alkynes and azides (as porphyrin terminal substituents) has emerged as one of the most effective tools, since it can be conducted in mild conditions, using a variety of solvents and resulting in the formation of the desired products in high yields, independently of the steric and electronic properties of the starting reagents (both electron-rich or electron-deficient substrates can be used).[60, 62, 63] Cu-catalyzed Huisgen 1,3-dipolar cycloaddition between azide- and acetylene-containing derivatives is the most effective reaction of this type which has led to a variety of porphyrin, phthalocyanine and other chromophore containing systems.[64-70] The 1,2,3-triazole bridge that results from such reactions has been proved to be very efficient for energy transfer in donor-acceptor systems.[71, 72] Also, according to literature reports, the measured efficiencies for a variety of mono-carboxylphenyl triaryl porphyrins have shown values from 0.5 to 3% in standard DSSCs.[73-75] Consequently, the solar cell performance of the single porphyrin dyes is expected to be lower than the performance of the final dyads. Herein, we describe the syntheses of two 1,2,3-triazole bridged porphyrin dyads, **9** and **11** (Scheme 1), synthesized under "click" reaction conditions, which containing terminal carboxylic acid groups for attachment to the TiO_2 surface of DSSCs. To the best of our knowledge, this is the first time "click" reaction

derived porphyrin dyad that are used as sensitizers in DSSCs. Nevertheless, to investigate the influence of the spacer (length) between the donor and acceptor parts of the sensitizing dye, the two derivatives **9**, **11** were synthesized. The difference between derivative **9** and **11** is due to the longer distance of the two porphyrin rings, as well to the presence of the small and non-conjugated aliphatic chain (C4) between them. The **9** and **11** sensitized solar cells resulted in PCE values of 3.82 and 5.16%, respectively. The enhanced photovoltaic performance of the latter solar cell is attributed to its better photovoltaic parameters, which are related to the stronger absorption profile of its sensitizing dye (dyad **11** with the shorter triazole containing bridge), higher dye loading onto the TiO_2 surface, longer electron lifetime and reduced recombination between injected electrons and electrolyte.

EXPERIEMENTAL DETAILS

Materials and techniques. All manipulations were carried out using standard Schlenk techniques under nitrogen atmosphere. 5-Bromovaleryl chloride, $Zn(CH_3COO)_2 \cdot 2H_2O$, NaN_3, $NaNO_2$, $NaHCO_3$, CuI, $CuSO_4$, sodium ascorbate, Trifluoroacetic acid (TFA), Na_2SO_4, KOH and other chemicals and solvents were purchased from usual commercial sources and used as received, unless otherwise stated. Dichloromethane (CH_2Cl_2) was distilled from CaH_2, tetrahydrofuran (THF) was distilled from Na/benzophenone, while triethylamine (Et_3N) was distilled and kept over activated 3 Å molecular sieves for 24 h prior use. Acetonitrile (CH_3CN) was kept over activated 3 Å molecular sieves for 24 h prior use. 5-(4-methylperoxyphenyl)-15-(4-aminophenyl)-10,20-bis(2,4,6-trimethylphenyl)porphyrin (**1**) and 5-(4-prop-2-ynyloxyphenyl)-10,15,20-triphenylporphyrin (**7**) were prepared according to literature procedures.[52, 76]

NMR spectra. NMR spectra were recorded on Bruker AVANCE III-500 MHz and Bruker DPX-300 MHz spectrometers using solutions in deuterated solvents and the solvent peak was chosen as the internal standard.

Mass spectra. High-resolution mass spectra (HRMS) were recorded on a Bruker UltrafleXtreme MALDI-TOF/TOF spectrometer, using trans-2-[3-(4-tert-Butylphenyl)-2-methyl-2-propenylidene]malononitrile as Matrix.

Photophysical measurements. UV-vis absorption spectra were measured on a Shimadzu UV-1700 spectrophotometer using 10 mm path-length cuvettes. Emission spectra were measured on a JASCO FP-6500 fluorescence spectrophotometer equipped with a red sensitive WRE-343 photomultiplier tube (wavelength range 200-850 nm).

Synthesis of [5-(4-methoxycarbonylphenyl)-15-(4-aminophenyl)-10,20-bis(2,4,6-trimethylphenyl)porphyrinato] zinc (2). To a CH_2Cl_2 solution (20 mL) of **1** (50 mg, 0.065 mmol) a MeOH solution (3 mL) of $Zn(CH_3COO)_2 \cdot 2H_2O$ (204 mg, 1 mmol) was added and the reaction mixture was stirred at room temperature overnight. The volatiles were removed under reduced pressure and, after diluted in CH_2Cl_2, the residue was purified by column chromatography (silica gel, CH_2Cl_2) resulting in 48 mg of **2** (yield: 90%). HRMS (MALDI-TOF): *m*/*z* calcd. for $C_{52}H_{44}N_5O_2Zn$ $[M+H]^+$ 834.2787, found 834.2790. Anal. Calcd for $C_{52}H_{43}N_5O_2Zn$: C, 74.77; H, 5.19; N, 8.38; Found: C, 74.83; H 5.25; N 8.30.

Synthesis of [5-(4-methoxycarbonylphenyl)-15-[4-(5-bromopentanamidophenyl)]-10,20-bis(2,4,6-trimethylphenyl)porphyrinato] zinc (3). To a solution of **2** (50 mg, 0.060 mmol) in dry CH_2Cl_2 (3 mL) and dry Et_3N (0,1 mL), 5-bromovaleryl chloride (45 µL 0.336 mmol) was added and the reaction mixture was stirred at 40°C for 3.5 hours. The solvent was removed under reduce pressure and CH_2Cl_2 (40 mL) were added. The organic phase was washed with H_2O (2 x 30 mL) separated and dried over anhydrous Na_2SO_4. The crude product was purified by column chromatography (silica gel, CH_2Cl_2) yielding 42 mg of **3**

(yield: 70%). ^{1}H NMR (300 MHz, DMSO-d^{6}): δ 10.30 (s, 1H), 8.77 (d, *J* = 4.4 Hz, 2H), 8.69 (d, *J* = 5.5 Hz, 2H), 8.57 (m, 4H), 8.35 (m, 4H), 8.10 (d, *J* = 7.9 Hz, 2H), 8.00 (d, *J* = 8.3 Hz, 2H), 7.31 (s, 4H), 4.03 (s, 3H), 3.66 (m, 2H), 2.57 (s, 6H), 2.54 (m, 2H), 1.96 (m, 2H), 1.85 (m, 2H), 1.78 (s, 12H). ^{13}C NMR (75 MHz, DMSO): δ 171.16, 167.49, 149.39, 149.06, 148.90, 148.57, 147.72, 139.04, 138.66, 138.32, 137.14, 136.83, 134.47, 134.38, 132.47, 134.38, 132.10, 131.52, 130.32, 130.01, 128.58, 127.21, 127.28, 119.83, 118.13, 117.84, 117.06, 52.32, 35.50, 34.81, 31.83, 23.84, 21.34, 20.98 ppm. HRMS (MALDI-TOF): *m*/*z* calcd. for $C_{57}H_{50}BrN_5O_3Zn$ $[M]^+$ 995.2388, found 995.2391. Anal. Calcd for $C_{57}H_{50}BrN_5O_3Zn$: C, 68.58; H 5.05; N 7.02. Found: C, 68.63; H 5.01; N 7.05.

Synthesis of [5-(4-methoxycarbonylphenyl)-15-[4-(5-azidopentanamidophenyl)]-10,20-bis(2,4,6-trimethylphenyl)porphyrinato] zinc (4). To a THF solution (40 mL) of **3** (50 mg, 0.050 mmol) an aqueous solution (4 mL) of NaN_3 (325 mg, 5 mmol) was added and the reaction mixture was refluxed for 4 hours. Upon removal of the solvents under reduced pressure, distilled H_2O (30 mL) and CH_2Cl_2 (30 mL) were added, and the organic layer was separated and dried over anhydrous Na_2SO_4. Purification of the crude product by column chromatography (silica gel, CH_2Cl_2/EtOH = 99/1) resulted in the isolation of 38 mg of **4** (yield: 79%). ^{1}H (500 MHz, DMSO-d^{6}): δ 10.31 (s, 1H), 8.77 (d, *J* = 4.6 Hz, 2H), 8.69 (d, *J* = 4.6 Hz, 2H), 8.57 (m, 4H), 8.35 (m, 4H), 8.10 (d, *J* = 8.5Hz, 2H), 8.01 (d, *J* = 8.5Hz, 2H), 7.31 (s, 4H), 4.03 (s, 3H), 3.46 (m, 2H), 2.57 (s, 6H), 2.53 (m, 2H), 1.80 (m, 2H), 1.77 (s, 12H), 1.71 (m, 2H). ^{13}C NMR (125 MHz, DMSO): δ 171.25, 166.52, 149.08, 148.91, 148.59, 147.76, 139.07, 138.71, 138.34, 137.14, 136.86, 134.50, 134.41, 132.14, 131.55, 130.35, 130.05, 128.57, 127.54, 127.31, 119.86, 118.16, 117.87, 117.07, 52.36, 50.49, 35.95, 27.97, 22.44, 21.38, 21.01. HRMS (MALDI-TOF): *m*/*z* calcd. for $C_{57}H_{50}N_8O_3Zn$ $[M]^+$ 958.3297, found 958.3303. Anal. Calcd for $C_{57}H_{50}N_8O_3Zn$: C, 71.28; H 5.25; N 11.67. Found: C, 71.23; H 5.21; N 11.72.

Synthesis of 5-(4-methoxycarbonylphenyl)-15-(4-azidophenyl)-10,20-bis(2,4,6-trimethylphenyl) porphyrin (5). To a TFA solution (1 mL) of **1** (100 mg, 0.130 mmol) at 0 ^{o}C an aqueous solution (0.5 mL) of $NaNO_2$ (30 mg, 0.435) was added. After stirring for 10 min at 0^{o}C, an aqueous solution (0.5 mL) of NaN_3 (50 mg, 0.769 mmol) was added and the reaction mixture was further stirred for 45 min. Next, CH_2Cl_2 (30 mL) and $NaHCO_3$ (30 mL) were added, and the organic layer was separated and dried over anhydrous Na_2SO_4. The crude product was purified by column chromatography (silica gel, CH_2Cl_2) yielding 83 mg of **5** (yield: 80%). ^{1}H NMR (500 MHz, $CDCl_3$): δ 8.79 (d, *J* = 4.7 Hz, 2H), 8.75 (d, *J* = 4.7 Hz, 2H), 8.72 (m, 4H), 8.44 (d, *J* = 8.4Hz, 2H), 8.32 (d, *J* = 8.4Hz, 2H), 8.21 (d, *J* = 8,5Hz, 2H), 7.43 (d, *J* = 8.5Hz, 2H), 7.29 (s, 4H), 4.11 (s, 3H), 2.64 (s, 6H), 1.85 (s, 12H), -2.62 (s,2H). ^{13}C NMR (125 MHz, $CDCl_3$): δ 167.51, 146.99, 139.99, 139.49, 138.81, 138.39, 138.00, 135.79, 134.68, 131.24, 130.55, 129.66, 128.06, 127.95, 118.82, 118.61, 118.09, 117.60, 52.58, 21.78, 21.62 ppm. HRMS (MALDI-TOF): *m/z* calcd. for $C_{52}H_{45}N_5O_2$ $[M-2N+2H]^+$ 771,3573 found 771,3578. Anal. Calcd for $C_{52}H_{43}N_7O_2$: C, 78.27; H 5.43; N 12.29. Found: C, 78.30; H 5.40; N 12.26.

Synthesis of [5-(4-methoxycarbonylphenyl)-15-(4-azidophenyl)-10,20-bis(2,4,6-trimethylphenyl)porphyrinato] zinc (6). A MeOH solution (3 mL) of $Zn(CH_3COO)_2{\cdot}2H_2O$ (204 mg, 1 mmol) was added to a CH_2Cl_2 solution (20 mL) of **5** (50 mg, 0.063 mmol) and the reaction mixture was stirred at room temperature overnight. After removing the volatiles under reduced pressure, the residue, after diluted in CH_2Cl_2, was purified by column chromatography (silica gel, CH_2Cl_2) resulting in 49 mg of **6** (yield: 90%). ^{1}H NMR (500 MHz, $CDCl_3$): δ 8.87 (d, *J* = 4.6 Hz, 2H), 8.83 (d, *J* = 4.6 Hz, 2H), 8.80 (m, 4H), 8.41 (d, *J* = 8.1 Hz, 2H), 8.32 (d, *J* = 8.1 Hz, 2H), 8.22 (d, *J* = 8,2 Hz, 2H), 7.39 (d, *J* = 8.3 Hz, 2H), 7.29 (s, 4H), 4.09 (s, 3H), 2.64 (s, 6H), 1.83 (s, 12H). ^{13}C NMR (125 MHz, $CDCl_3$): δ 167.57, 150.23, 150.22, 150.16, 149.70, 147.87, 139.69, 139.65, 139.36, 139.01, 137.74, 135.68,

134.60, 132.34, 132.13, 131.27, 131.14, 129.42, 127.90, 127.85, 119.77, 119.50, 119.04, 117.42, 52.52, 21.80, 21.62 ppm. HRMS (MALDI-TOF): *m*/*z* calcd. for $C_{52}H_{43}N_5O_2Zn$ [M-2N+2H]$^+$ 833.2708, found 833.2713. Anal. Calcd for $C_{52}H_{41}N_7O_2Zn$: C, 72.51; H 4.80; N 11.38. Found: C, 74.60; H 4.85; N 11.27.

Synthesis of porphyrin dyad 8. *"Click" reaction.* Equimolar amounts of porphyrin **4** (30 mg, 0.031 mmol) and porphyrin **7** (23 mg, 0.031 mmol) were dissolved in a 3:1 mixture of $CHCl_3/H_2O$ (6 mL) under nitrogen atmosphere. Sodium ascorbate (3.7 mg, 0.019 mmol) and $CuSO_4.5H_2O$ (1.6 mg, 0.006 mmol) were added and the reaction mixture was stirred at 50^{o}C for 72 hours. Upon reaction completion, a $CHCl_3/H_2O$ mixture (40/40 mL) was added. The organic layer was extracted and dried over anhydrous Na_2SO_4. The crude product was purified by column chromatography (silica gel, CH_2Cl_2/EtOH = 99/1) resulting in the formation of 22 mg of **8** (yield: 42%). ^{1}H (500 MHz, DMSO-d^6): δ 10.37 (s, 1H), 8.80 (d, *J* = 4.5 Hz, 2H), 8.74 (m, 8H), 8.65 (d, *J* = 4.5 Hz, 2H), 8.53(d, *J* = 4.4 Hz, 4H), 8.34 (s, 1H), 8.31 (d, *J* = 8.1 Hz, 2H), 8.28 (d, *J* = 7.9 Hz, 2H), 8.11 (m, 6H), 8.06 (m, 4H), 7.99 (d, *J* = 8.1 Hz, 2H), 7.56 (m, 9H), 7.40 (d, *J* = 7.8 Hz, 2H), 7.18 (s, 4H), 5.37 (s, 2H), 4.55 (m, 2H), 3.98 (s, 3H), 2.54 (m, 2H), 2.45 (s, 6H), 2.04 (m, 2H), 1.74 (m, 2H), 1.69 (s, 12H). ^{13}C NMR (125 MHz, DMSO-d^6): δ 171.90, 167.11, 158.07, 150.09, 149.86, 149.74, 149.67, 149.55, 149.39, 149.06, 148.16, 148.16, 143.26, 143.12, 139.43, 139.02, 138.77, 137.73, 137.35, 135.68, 134.93, 134.89, 134.58, 132.65, 132.15, 132.01, 130.82, 130.53, 129.01, 127.95, 127.82, 127.05, 125.21, 120.74, 120.66, 120.28, 118.69, 118.37, 117.71, 113.32, 61.78, 52.84, 49.84, 36.30, 29.94, 22.72, 21.76, 21.38 ppm. HRMS (MALDI-TOF): *m*/*z* calcd. for $C_{104}H_{80}N_{12}O_4Zn_2$ [M]$^+$ 1688.5008, found 1688.5012. Anal. Calcd for $C_{104}H_{80}N_{12}O_4Zn_2$: C, 73.80; H, 4.76; N, 9.93. Found: C, 73.85; H 4.79; N 9.83.

Synthesis of porphyrin dyad 9. *Ester hydrolysis.* To a solution of **8** (35 mg, 0.021 mmol) in 22 mL of a THF/MeOH mixture (2:1), an aqueous solution (7 mL) of KOH (300 mg, 5.35

mmol) was added. The reaction mixture was stirred at room temperature overnight. The solvents were evaporated under reduced pressure and distilled H_2O (10 mL) was added to the resulting residue. Acidification of the mixture by using HCl(aq) 1 M resulted in the precipitation of a solid which was filtered, washed with distilled H_2O and dried yielding 32 mg of porphyrin dyad **9** (91%). ^{1}H (500 MHz, DMSO-d^6): δ 13.18 (s, 1H), 10.35 (s, 1H), 8.83 (d, *J* = 4.6 Hz, 2H), 8.77 (m, 8H), 8.69 (d, *J* = 4.6 Hz, 2H), 8.56 (m, 4H), 8.50 (s, 1H), 8.32 (m, 4H), 8.17 (m, 6H), 8.11 (d, *J* = 7.5 Hz, 2H), 8.03 (d, *J* = 8.4 Hz, 2H), 7.77 (s, 9H), 7.48 (d, *J* = 8.6 Hz, 2H), 7.26 (s, 4H), 6.58 (s, 2H), 5.46 (s, 2H), 4.60 (t, *J* = 6.98Hz, 2H), 2.58 (t, *J* = 5.5Hz, 2H), 2.53 (s, 6H), 2.08 (m, 2H), 1.80 (m, 2H), 1.75 (s, 12H) ppm. ^{13}C NMR (125 MHz, DMSO): δ 171.68, 168.08, 158.22, 150.13, 149.90, 149.76, 149.69, 149.55, 149.40, 149.16, 147.80, 143.31, 143.24, 143.18, 139.56, 139.18, 138.82, 137.32, 135.74, 135.70, 134.92, 134.85, 134.63, 132.62, 132.19, 132.04, 131.98, 130.80, 130.53, 130.79, 128.01, 127.94, 127.05, 125.25, 120.73, 120.69, 120.65, 120.31, 118.61, 117.59, 113.34, 61.98, 49.84, 36.98, 30.04, 22.77, 21.87, 21.47 ppm. HRMS (MALDI-TOF): *m*/*z* calcd. for $C_{103}H_{78}N_{12}O_4Zn_2$ $[M]^+$ 1674.4852, found 1674.4857. Anal. Calcd for $C_{103}H_{78}N_{12}O_4Zn_2$ C, 73.70; H, 4.68; N, 10.01. Found: C, 73.77; H 4.72; N 10.00.

Synthesis of porphyrin dyad 10. *"Click" reaction*. Equimolar amounts of porphyrin **6** (30 mg, 0.034 mmol) and porphyrin **7** (25 mg, 0.034 mmol) were dissolved in a 1:1 mixture of THF/CH_3CN (5 mL) under nitrogen atmosphere. Next, CuI (6 mg, 0.032 mmol) was added and the reaction mixture was stirred at room temperature for 12 hours. Upon reaction completion, the volatiles were removed under reduced pressure and the crude solid, after diluted in CH_2Cl_2, was purified by column chromatography (silica gel, CH_2Cl_2) yielding the 22 mg of **10** (yield: 41%). ^{1}H (500 MHz, $CDCl_3$): δ 9.00 (s, 4H), 9.95 (m, 4H), 8.82 (m, 6H), 8.76 (d, *J* = 4.6 Hz, 2H), 8.40 (d, *J* = 8 Hz, 2H), 8.34 (d, *J* = 7.9 Hz, 2H), 8.27 (m, 6H), 8.21 (d, *J* = 8.0 Hz, 2H), 8.06 (d, *J* = 7.9 Hz, 2H), 7.74 (m, 6H), 7.67 (m, 3H), 7.41 (s, 1H), 7.39

(m, 2H), 7.30 (s, 4H), 6.82 (d, J = 7.6 Hz, 2H), 4.05 (s, 3H), 2.96 (s, 2H), 2.64 (s, 6H), 1.85 (s, 12H) ppm. ^{13}C NMR (125 MHz, DMSO-d^6): δ 167.54, 157.36, 150.64, 150.49, 150.32, 150.26, 149.79, 149.75, 148.01, 144.07, 143.41, 139.36, 139.13, 137.74, 136.33, 136.12, 135.47, 135.34, 134.74, 134.65, 132.23, 132.06, 131.91, 131.31, 129.40, 127.87, 127.48, 126.58, 121.29, 121.10, 120.56, 119.82, 119.27, 119.10, 118.23, 118.03, 112.91, 67.07, 52.46, 21.83, 21.62 ppm. HRMS (MALDI-TOF): m/z calcd. for $C_{99}H_{71}N_{11}O_3Zn_2$ $[M]^+$ 1589.4324, found 1589.4326. Anal. Calcd for $C_{99}H_{71}N_{11}O_3Zn_2$: C, 74.62; H, 4.49; N, 9.67. Found: C, 74.70; H 5.46; N 9.60.

Synthesis of porphyrin dyad 11. *Ester hydrolysis.* To a solution of **10** (50 mg, 0.032 mmol) in 22 mL of THF/MeOH mixture (2:1), an aqueous solution (7 mL) of KOH (300 mg, 5.35 mmol) was added and the mixture was stirred at room temperature overnight. The solvents were evaporated under reduced pressure and distilled H_2O (10 mL) was added to the resulting residue. After acidification of the mixture by addition of HCl (aq) 1 M, the product was precipitated, filtered, washed with distilled H_2O and dried resulting in 46 mg of porphyrin dyad **11** (yield: 91%). ^{1}H (500 MHz, DMSO-d^6): δ 13.1 (s, 1H), 9.4 (s, 1H), 8.88 (d, J = 4.6 Hz, 2H), 8.83 (d, J = 4.5 Hz, 2H), 8.80 (d, J = 4.5 Hz, 2H), 8.78 (s, 4H), 8.74 (d, J = 4.6Hz, 2H), 8.64 (d, J = 4.6Hz, 2H), 8.62 (d, J = 4.5 Hz, 2H), 8.46 (d, J = 8.1 Hz, 2H), 8.41 (d, J = 8.1 Hz, 2H), 8.35 (m, 4H), 8.18 (m, 8H), 7.79 (s, 9H), 7.55 (d, J = 8.3 Hz, 2H), 7.32 (s, 4H), 5.63 (s, 2H), 2.58 (s, 6H), 1.80 (s, 12H) ppm. ^{13}C NMR (125 MHz, DMSO): δ 158.16, 150.17, 149.81, 149.75, 149.69, 149.65, 149.53, 149.28, 147.73, 144.74, 143.27, 139.53, 138.87, 137.41, 135.93, 135.81, 135.78, 134.87, 134.66, 132.36, 132.24, 132.08, 130.94, 130.31, 128.07, 128.00, 127.92, 127.07, 123.83, 120.79, 120.69, 119.10, 118.90, 118.82, 118.75, 113.44, 61.89, 21.92, 21.50 ppm. HRMS (MALDI-TOF): m/z calcd. for $C_{98}H_{69}N_{11}O_3Zn_2$ $[M]^+$ 1575.4168, found 1575.4173. Anal. Calcd for $C_{98}H_{69}N_{11}O_3Zn_2$: C, 74.52; H, 4.40; N, 9.76. Found: C, 74.55; H 4.35; N 9.80.

Electrochemistry: Cyclic and square wave voltammetry experiments were carried out at room temperature using an AutoLab PGSTAT20 potentiostat and appropriate routines available in the operating software (GPES, version 4.9). Measurements were carried out in freshly distilled and deoxygenated THF, with scan rate 100 mV/s, with a solute concentration of 1.0 mM in the presence of tetrabutylammonium tetrafluoroborate (0.1 M) as supporting electrolyte. A three-electrode cell setup was used with a platinum working electrode, a saturated calomel (SCE) reference electrode, and a platinum wire as counter electrode. The system was calibrated by ferrocene.

Computational Methods: Density functional theory (DFT) calculations[77] were performed using the GAUSSIAN 03 program suite.[78] Gas phase geometry optimizations were carried out by employing Becke three parameter exchange in conjunction with Lee-Yang-Parr correlation functional (B3LYP).[79, 80] For the geometry optimizations, the LANL2DZ basis set was used for Zn atoms and the 6-31G(d) basis sets for lighter atoms. The input geometries were modeled using the ChemCraft software.[81] The optimized minimum-energy structures were verified as stationary points on the potential energy surface by vibrational frequency analysis calculation. Computed structures and molecular orbitals were visualized and analyzed by ChemCraft software.

Preparation of TiO_2 electrodes and DSSCs. The DSSCs were fabricated with electrodes based on fluorine-doped tin oxide (FTO)-coated glass substrates, which were pre-cleaned with deionized water, acetone, and ethanol and then dried in air. The working electrodes for the DSSC were prepared by firstly forming a blocking layer from 0.2 M di-isopropoxy titanium bis (acetylacetone) in isopropanol by spray pyrolysis. This was then followed by the deposition of a nano-crystalline layer of TiO_2 using the doctor blade technique using dye sol TiO_2 paste (DSL 18NR-T) on a pre-cleaned FTO coated glass substrate. The TiO_2 coated FTO electrodes were heated at 500^{o}C for 30 min. The TiO_2 electrodes were then dipped in

0.02 M aqueous $TiCl_4$ for 20 minutes, rinsed with water and ethanol and annealed at 500°C for 20 min. The thickness of the TiO_2 electrode was measured using a thin film thickness measurement system (Nano calc XR Ocean Optics Germany) and found to be in the range 10-12 μm. Finally, it was immersed in a porphyrin solution (200 μM in THF) for 12 h to give the porphyrin-sensitized TiO_2 working electrode. The platinum wire counter electrode was prepared by spin-coating drops of a H_2PtCl_6 solution onto a FTO-coated glass substrate and heating at 350°C for 15 min. The DSSCs were assembled by separating the working electrode from the counter electrode by a 20 μm thick Surlyn hot-melt gasket. In the space between the working and counter electrodes, the electrolyte [consisting of 0.05 M I_2, 0.5 M LiI, 0.6 M dimethylpropyl-benzimidiazole iodide, 0.5 M 4-tert-butylpyridine in an acetonitrile solution] was introduced through a hole and sealed with Surlyn.

Photovoltaic measurements. The current-voltage (*J-V*) characteristics of the DSSCs under illumination were measured by a Keithley source meter and a solar simulator coupled with a 150 W xenon lamp and an AM optical filter to give an illumination intensity of 100 mW cm^{-2} at the DSSC surface. The electrochemical impedance spectra (EIS) in the dark were recorded by using an electrochemical workstation (Auto lab PGSTAT) with a frequency response analyzer. The frequency range was from 10 mHz to 100 KHz, and an ac potential of 10 mV was used. A dc bias equivalent to the open-circuit voltage of the DSSC was applied. The impedance data were analyzed by using Z-View software with an appropriate equivalent circuit. The incident photon to current conversion efficiency (IPCE) was measured as a function of wavelength with a xenon lamp, monochromator, and Keithley source meter at 10 mW cm^{-2}. The intensity calibration for the IPCE measurement was performed by using a standard silicon photodiode.

RESULTS AND DISCUSSION

Structures, synthesis and characterization. As shown in Scheme 1, dyads **9** and **11** consist of two zinc-metallated porphyrin units which are covalently linked at their peripheries by1,2,3- triazole containing bridges of different lengths. One of the porphyrin units of each dyad is functionalized at the meso position opposite to the triazole bridge by a benzoic acid moiety, which can function as anchoring group for attachment onto the TiO_2 surface of DSSCs.

The synthesis of the two dyads **9** and **11**, depicted in Scheme 2, is based on the utilization of click-type reactions. The dyads were obtained via click-reactions which are Cu-catalyzed versions of the Huisen 1,3-dipolar cycloaddition between an alkyne and an azide groups that lead to the formation of a 1,2,3-triazole ring. Therefore, the first step of their syntheses involved the preparation of the corresponding terminal alkyne and azide containing porphyrins. The former, i.e. 5-(4-prop-2-ynyloxyphenyl)-10,15,20-triphenylporphyrin (**7**), a reagent used for the syntheses of both dyads, was prepared according to previously published procedures. Two different azide containing porphyrins were used, **4** and **6**, which differ in the positioning of the azide group relative to the porphyrin framework. In porphyrin **4**, the azide group is located at the end of a six-member, heteroatom containing, aliphatic side chain, which is attached to a *meso* phenyl group of the porphyrin unit. The synthesis of this compound started from the reaction of porphyrin **1** with excess of $Zn(CH_3COO)_2 \cdot 2H_2O$ which yielded the metallated porphyrin **2**. The reaction of **2** with 5-bromovaleryl chloride in CH_2Cl_2 in the presence of Et_3N, resulted in the formation of the alkyl-bromide containing porphyrin adduct **3**, which, after its purification and isolation, further reacted with NaN_3, to afford the azide containing porphyrin **4**. The analogous porphyrin **6** containing the azide group at the periphery of a *meso* phenyl group substitutent was prepared from the reaction of the free-base porphyrin **1** with NaN_3, followed by metallation with $Zn(CH_3COO)_2 \cdot 2H_2O$.

"Click" reaction between the azide containing porphyrin **4** and the terminal alkyne containing porphyrin **7**, catalyzed by $CuSO_4 \cdot 5H_2O$ and sodium ascorbate, in a mixture of $CHCl_3/H_2O$, resulted in the formation of the triazole-bridged porphyrin dyad **8**. The most noticeable feature in the ^{1}H NMR spectrum of **8** is the appearance of a characteristic signal at 8.40 ppm which is assigned to the H of the newly formed triazole ring. Finally, basic hydrolysis of the methyl ester group of **8**, followed by aqueous work-up, resulted in the formation of the desired dyad **9**. In the ^{1}H NMR spectrum of **9**, it should be noticed the absence of any signal due to the methyl-ester H's and the appearance of a signal assigned to the carboxylic acid H at 13.18 ppm, while in its ^{13}C NMR the characteristic signal of the secondary carbon atom of the triazole ring and the carboxylic acid group, which appear at 125.25 and 168.08 ppm respectively.

The synthesis of porphyrin dyad **11** was achieved in a similar fashion except that in this case the click-reaction affording the triazole-bridged porphyrin dyad **10** was catalyzed by CuI in THF. The use of the $CuSO_4$/ascorbate catalytic system employed in the aforementioned click-reaction did not afford the desired dyad. Apparently, this can be attributed to the different nature of the azide group. The fact that the reaction does not lead to the desired product, it is well known according to the literature data.[64] More precisely, when the azide group is located on the phenyl ring of the porphyrin the reaction does not take place in the presence of CuSO4 and Na ascorbate. That is the reason why we had to use the described experimental procedure[66] for the synthesis of the desired product (**10**). The final product **11** was obtained after basic hydrolysis of the methyl ester group of **10**. All the synthesized compounds were fully characterized by ^{1}H NMR, ^{13}C NMR and MALDI-TOF spectrometry.

Photophysical studies. The UV-vis absorption spectra of porphyrin dyads **9** and **11** in THF solutions are shown in Figure 1a (black and red color lines, respectively). The spectra of both compounds exhibit the typical absorption bands of zinc-metallated porphyrins, with an

intense Soret band in the 420-430 nm and two moderate Q-bands observed in the 555-600 nm range (Table 1), which are attributed to π-π* electronic transitions within the porphyrin framework. No other spectral features are observed, which gives an indication that there are no intramolacular interactions between the porphyrin units through the triazole bridges in the ground states of both porphyrin dyads.

In Figure 1b are depicted the UV-vis absorption spectra of porphyrin dyads **9** and **11** adsorbed on TiO_2 films (black and red color lines, respectively). They show the usual porphyrin Soret and Q bands, but, compared to the corresponding absorption spectra in solution, these are broadened and slightly shifted to longer wavelengths. In general, when anchored onto the TiO_2 surface, porphyrins form either face-to-face π-aggregates (*H*-aggregates), which usually results in absorption bands shifted to shorter wavelengths (blue-shifted) relative to the corresponding bands in solution spectra, or edge-to-edge π-aggregates (*J*-aggregates), which usually give red-shifted (to longer wavelengths) absorption bands. The observed red-shifted bands of both **9** and **11** provide an indication of *J*-type aggregation of the porpyrin dyads onto the TiO_2 surface. It is worth-mentioning that dyad **11** adsorbed onto the TiO_2 film exhibits stronger absorption bands than dyad **9**, which suggests a larger amount of dye adsorbed onto TiO_2 film. Furthermore, the broad, red-shifted and higher intensity Q-bands of both dyads **9** and **11** adsorbed onto the TiO_2 surface indicate a strong electronic coupling between the dyads and the TiO_2 surface as well as enhanced light harvesting capacity of the low energy photons, which is highly desirable for efficient sensitizers in DSSCs.

Based on the onset absorption edges λ_{onset} of the Q bands of dyads **9** and **11** adsorbed on thin TiO_2 films, which are found to be 646 and 626 nm, respectively, the corresponding optical band gap energies E_g^{opt}, calculated from the expression

$$E_g^{opt} = 1240 \ / \ \lambda_{onset}$$

were found to be 1.92 and 1.98 eV, respectively (Table 1).

Electrochemical studies. In order to evaluate the feasibility of electron transfer from the photo-excited dyads **9** and **11** into the TiO_2 CB as well as their regeneration by the I^-/I_3^- couple of the electrolyte in the corresponding DSSCs, the electrochemical properties of the two dyads were investigated by cyclic voltammetry (Figure 2) and square-wave voltammetry measurements (Figure S33 in Supporting Information). The relevant electrochemical data are summarized in Table 2. Porphyrin dyad **9** exhibits one reversible oxidation process at E_{ox}^1 = +0.93 V and one reversible reduction process at E_{red}^1 = -1.48 V, vs SCE which corresponds to the overlapping oxidation and reduction of both porphyrin units. Porphyrin dyad **11** exhibits similar reversible processes at E_{ox}^1 = +1.02 V and E_{red}^1 = -1.42 V vs SCE. These data are typical for *meso* tetra-aryl substituted Zn-metallated porphyrins[82] and suggest that there is negligible electronic interaction between the two porphyrin units in the ground states of both dyads.

In a DSSC, for efficient electron injection of the photo-excited sensitizer into the TiO_2 CB, the lowest unoccupied molecular orbital (LUMO) energy level of the sensitizer (which corresponds to its first reduction potential E_{red}^1) should be higher than the TiO_2 CB edge (-0.74 V *vs* SCE). Both compounds **9** and **11** display E_{red}^1 values which are more negative than the TiO_2 CB, suggesting that there is sufficient driving force for electron injection from the photo-excited dyads into the TiO_2 CB ($\Delta G_{inj}<0$) (Figure 3). Furthermore, in order to ensure efficient regeneration of the sensitizer radical cation (after electron injection) in a DSSC, the highest occupied molecular orbital (HOMO) energy level of the sensitizer (which corresponds to its first oxidation potential E_{ox}^1) should be lower than the corresponding redox potential of the electrolyte redox couple used in the solar cell, i.e. I^-/I_3^- (+0.20 V *vs* SCE). The E_{ox}^1 values of both **9** and **11** are more positive than the electrolyte redox potential, and

therefore regeneration of the dyads, after electron injection, is thermodynamically feasible ($\Delta G_{reg}<0$).[83, 84]

The HOMO-LUMO band gaps E_g^{elec} for **9** and **11** estimated from electrochemical data were found to be 2.41 and 2.44 eV, respectively (Table 2), which are larger than the corresponding HOMO-LUMO band gaps E_g^{opt} estimated from photophysical measurements (Table 1). However, this is an ordinary characteristic of organic dyes of this type, which can be attributed to solvent effects.[85]

DFT Calculations. In order to gain insight into the molecular and electronic structures of dyads **9** and **11**, DFT calculations at the B3LYP/6-31G(d) level of theory were performed. Due to the fact that the total number of atoms of dyads is too large for DFT calculations in our computer cluster, the molecules were simplified by replacing the phenyl and 2,4,6-trimethylphenyl groups at the *meso* positions of the porphyrin units with H atoms, which should not have any influence on the HOMO and LUMO energy levels of the molecules.

The gas-phase geometry optimized structures of dyads **9** and **11** are depicted in Figure 4, while their optimized coordinates are provided in Tables S1 and S2 in Supporting Information. Both molecules adopt a "butterfly like" structure, in which the porphyrin units are attached as wings at the ends of the triazole-containing bridges. In **11**, the triazole ring is almost co-planar with the two bridging phenyl group forming a framework which is in a perpendicular orientation with respect to the two porphyrin units.

The electron density distributions of the frontier molecular orbitals of the two dyads and the corresponding energy levels are presented in Figure 5. The HOMO, HOMO-1 and HOMO-2 are close in energy. In both molecules, the electron density of the HOMOs is predominantly located on the unsubstituted porphyrin unit, with some additional contributions on the bridging phenyl groups. The LUMO is spread over the functionalized porphyrin unit, the terminal benzoic acid group and the bridging phenyl group, while the LUMO+1 is entirely

localized on the functionalized porphyrin unit. Consequently, both dyads could be described as "push-pull" D-π-A systems (D: donor, A: acceptor) and they have the potential to act as successful sensitizers in DSSCs, since the electron density distributions on HOMO, LUMO, and LUMO+1 is such that could promote intramolecular electron transfer, upon photoexcitation, from one porphyrin unit to the porphyrin with the carboxylic acid and, finally, injection into the TiO_2 CB. Nevertheless, intramolecular electron transfer is not expected to be very efficient. The non-planar orientation of the porphyrin units, the conjugation break caused by the twisted phenyl and triazole rings and the presence of sp^3 hybridized atoms (O and C) in the bridging units, together with the long distance between the two chromophore units weaken the electronic communication between the porphyrin π-systems. This is evident in the UV-vis absorption spectra, and electrochemical behavior of both dyads.

The calculated HOMO-LUMO gaps in THF solution of dyads **9** and **11** were found to be 2.793 and 2.744 eV, respectively, which are similar to the experimentally observed HOMO-LUMO gaps from electrochemistry experiments.

Photovoltaic properties. The **9** and **11** based DSSCs have been fabricated and their current-voltage (*J-V*) characteristics are shown in Figure 6 (black and red color lines, respectively), while the corresponding photovoltaic cell parameters, i.e. short circuit photocurrent (J_{sc}), open circuit voltage (V_{oc}), fill factor (*FF*), and power conversion efficiency (PCE), are compiled in Table 3. The solar cell employing porphyrin dyad **9** as sensitizer exhibits a PCE value of 3.82% (with J_{sc} = 9.36 mA/cm^2, V_{oc} = 0.62 V, and *FF* = 0.68) while the solar cell based on **11** gives a higher PCE value of 5.16% (with J_{sc} = 10.84 mA/cm^2, V_{oc} = 0.68 V, and *FF* = 0.70). In other words, the dyad with the shorter triazole containing bridge results in a higher PCE value than the dyad with the longer bridge.

One of the reasons for the higher PCE value of the **11** based solar cell is its higher J_{sc} value. Given that J_{sc} of a solar cell is related to its IPCE response, the different J_{sc} values of the two solar cells should be reflected on their respective IPCE spectra. The IPCE spectra of both devices, shown in Figure 7 (black and red color lines, respectively), resemble the absorption spectra of the dyads adsorbed on TiO_2 films, exhibiting characteristic peaks of moderate intensity in the 400-470, 540-580, and 600-740 nm ranges. However, the scattering by TiO_2 nanoparticles increases the photocurrent in the relatively weak absorption region.[86] The solar cell sensitized by **11** exhibits a stronger IPCE response than the solar cell sensitized by **9**, which is consistent with a higher J_{sc} value.

The IPCE of a DSSC is defined as

$$IPCE = LHE \times \varphi_{inj} \times \eta_c$$

where LHE is the the light harvesting efficiency, electron injection efficiency φ_{inj}, and charge collection efficiency η_c of the solar cell.[87] LHE depends on the absorption profile of the sensitizer and the amount of dye adsorbed on the TiO_2 surface and it is expressed as $1\text{-}10^{-\varepsilon\Gamma}$, where ε is the molar absorptivity of the dye and Γ is the molar concentration of dye loaded per surface area of the TiO_2 film. Therefore, the stronger IPCE response and the corresponding higher J_{sc} value of the **11** based solar cell should result from higher values of these two parameters. Indeed, as shown in Figures 1b and 7, dyad **11** adsorbed on TiO_2 displays a stronger absorption profile with a higher molar absorptivity value than **9**. Furthermore, the amount of dye per surface area or dye loading value (estimated spectroscopically by immersing the dye-sensitized TiO_2 films of thickness 12 μm into a 0.1 M NaOH solution in a 1:1 v/v mixture EtOH:THF and measuring the absorption spectra of the de-adsorbed dyes) for the **11** based solar cell was found to higher than the one for the **9** based solar cell (4.34×10^{-7} and 1.45×10^{-7} mol cm^{-2}, respectively).

The electron injection rate from the photo-excited dye into the TiO_2 CB influences the J_{sc} and, hence, the PCE value of a solar cell. This is strongly affected by dye-aggregation on the TiO_2 surface of the photoanode of the solar cell, since it increases the probability of relocation of a porphyrin excited states in neighboring porphyrin units (exiton quenching) decreasing the electron injection efficiency.[84, 88, 89] The only difference between the structures of dyads **9** and **11** is the length of the triazole containing bridge connecting the two porphyrin units. Since dyad **9** contains a longer bridge, it has higher flexibility than dyad **11**, and therefore it should be expected to have a higher tendency to resist dye aggregation, resulting in a higher PCE value. However, the results presented herein suggest that the different degrees of dye aggregation of the **9** and **11** based solar cells is not a factor that decisively differentiates their electron injection rates and their overall performances.

Furthermore, the ΔG_{inj} values of the two solar cells are similar, as estimated from the aforementioned electrochemistry data, indicating that there is essentially no difference in their corresponding driving forces available for electron injection.

Charge transport and recombination processes also play an important role in determining the PCE value of a DSSC. Aiming to get information about the relationship between these processes in the **9** and **11** based solar cells and the corresponding observed photovoltaic parameters, the electrochemical impedance spectra (EIS) of the two solar cells in dark conditions at a forward bias of 0.65 V were recorded.[90-92] In the Nyquist plots of EIS of the two devices are shown in Figure 8a (black and red color lines for the **9** and **11** sensitized solar cells, respectively). The plots for both devices comprise of three semicircles, which are associated with the charge transfer resistance at the counter electrode/electrolyte interface (in the high frequency region), charge recombination resistance at the TiO_2/dye/electrolyte interface (in the middle frequency region) and ion diffusion resistance in the electrolyte of the solar cell (in the low frequency region). The larger semicircle radius in the middle frequency

region for the DSSC sensitized by porphyrin dyad **11** indicates a higher charge recombination resistance for the former device which means that the charge recombination rate is slower for this device.

The Bode phase plots of EIS of **9** and **11** sensitized solar cells are shown in Figure 8b (black and red color lines, respectively). In both plots, the peak in the high frequency region corresponds to the charge transfer resistance at the counter electrode, while the peak in the lower frequency region is related to the charge recombination resistance. The frequency at the maximum (f_{peak}) of the latter peak can be used to calculate the electron lifetime (τ_e) of a solar cell.[93, 94] The electron lifetime (τ_e) values for the **9** and **11** based solar cells were calculated according to the relationship

$$\tau_e = \frac{1}{2\pi f_{max}}$$

and they were found to 22 and 31 ms, respectively. The longer electron lifetime for the latter device based on **11** is indicative of a more effective suppression of recombination between injected electrons and the electrolyte, and therefore to a reduced charge recombination rate, resulting in an enhanced V_{oc} value.[95]

CONCLUSIONS

We have synthesized two novel porphyrin dyads **9** and **11** consisted of two zinc-metallated porphyrin units, which are covalently linked through their *meso* phenyl groups by 1,2,3-triazole containing bridges of different lengths. Both dyads are also functionalized by a terminal carboxylic acid group. These were synthesized via "click" reactions, which are Cu-catalyzed Huisgen 1,3-dipolar cycloadditions between azide- and acetylene-containing porphyrins. Due to the different position of the azide group in the corresponding azide-containing porphyrins (either on aliphatic carbon chain or on phenyl group), the "click" reaction leading to the syntheses of the two dyads required the use of different catalytic

reactions conditions. UV-vis spectra and cyclic voltammetry measurements, as well as DFT calculations, revealed that there is negligible electronic interaction between the two porphyrin units in the ground states of both dyads, but the dyads possess frontier orbital energy levels which are suitable for use as sensitizers in DSSCs. Fabrication of the corresponding solar cells revealed that the device based on the dyad with the shorter triazole containing bridge (**11**) results in a better photovoltaic performance (3.82 and 5.16% for **9** and **11**, respectively). As demonstrated by the *J-V* curves and the IPCE and EI spectra of the two solar cells, the higher PCE value of the latter can be attributed to its enhanced short circuit current (J_{sc}) under illumination, its longer electron lifetime (τ_e) and more effective charge recombination resistance between injected electrons and the electrolyte, as well as its higher dye loading on the TiO_2 surface.

ASSOCIATED CONTENT

Supporting Information. Complementary data of ^{1}H NMR and ^{13}C NMR spectra of compounds **3-11**, cyclic voltammograms and square-wave voltammograms of dyads **9** and **11** and optimized coordinates from DFT calculations for **9** and **11.**

AUTHOR INFORMATION

Corresponding Authors.

* E-mail: coutsole@chemistry.uoc.gr (A.G.C.); gdsharma273@gmail.com (G.D.S.).

ACKNOWLEDGEMENTS

Financial support from the European Commission (FP7-REGPOT-2008-1, Project BIOSOLENUTI No. 229927) is greatly acknowledged. This research has also been co-financed by the European Union (European Social Fund) and Greek national funds

(Heraklitos II) through the Operational Program "Education and Lifelong Learning" of the National Strategic Reference Framework Research Funding Program (THALIS-UOA-MIS 377252. We are also thankful to Department of Physics, LNMIT, Jaipur and Material Science Research Laboratoty, MNIT, Jaipur for allowing fabricating the DSSCs and their characterization.

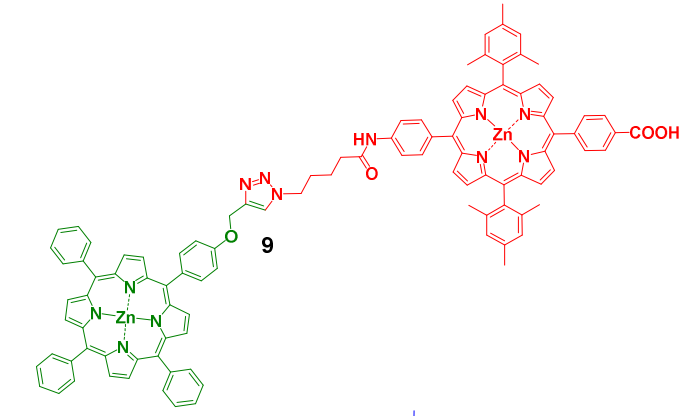

9

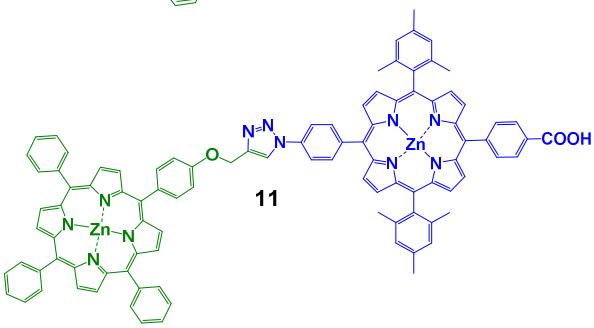

11

Scheme 1

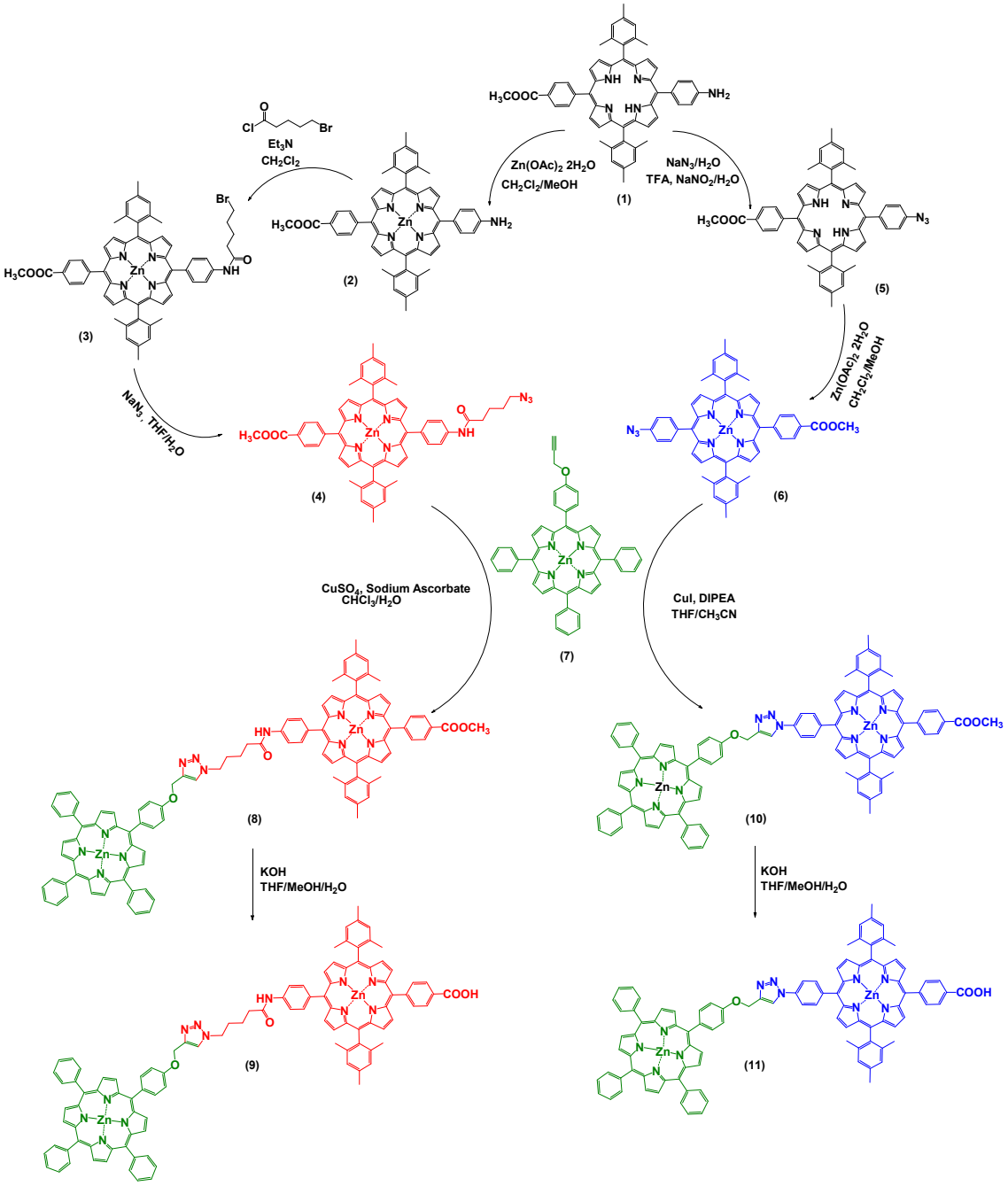

Scheme 2

Table 1. Photophysical data and calculated optical band gaps E_g^{opt} for **9** and **11**.

compound	absorption λ_{max} (ε)[a] / nm ($\times 10^3$ M^{-1} cm^{-1})	E_g^{opt} / eV
9	425 (628.3), 557 (14.4) and 598 (4.3)	1.92
11	426 (766.6), 556 (24.8) and 598 (6.5)	1.98

[a] at 298K in THF

Table 2. Electrochemical data of **9** and **11**.

compound	E_{ox}^{1} / V vs SCE	E_{red}^{1} / V vs SCE	E_{elec} / eV
9	0.93	-1.48	2.41
11	1.02	-1.42	2.44

Table 3. Photovoltaic parameters of DSSCs sensitized by **9** and **11**.

DSSC sensitized by	J_{sc} / mA cm^{-2}	V_{oc} / V	FF	PCE / %	dye loading / 10^{-7} mol cm^{-2}
9	9.36	0.62	0.68	3.82	1.45
11	10.84	0.68	0.70	5.16	4.34

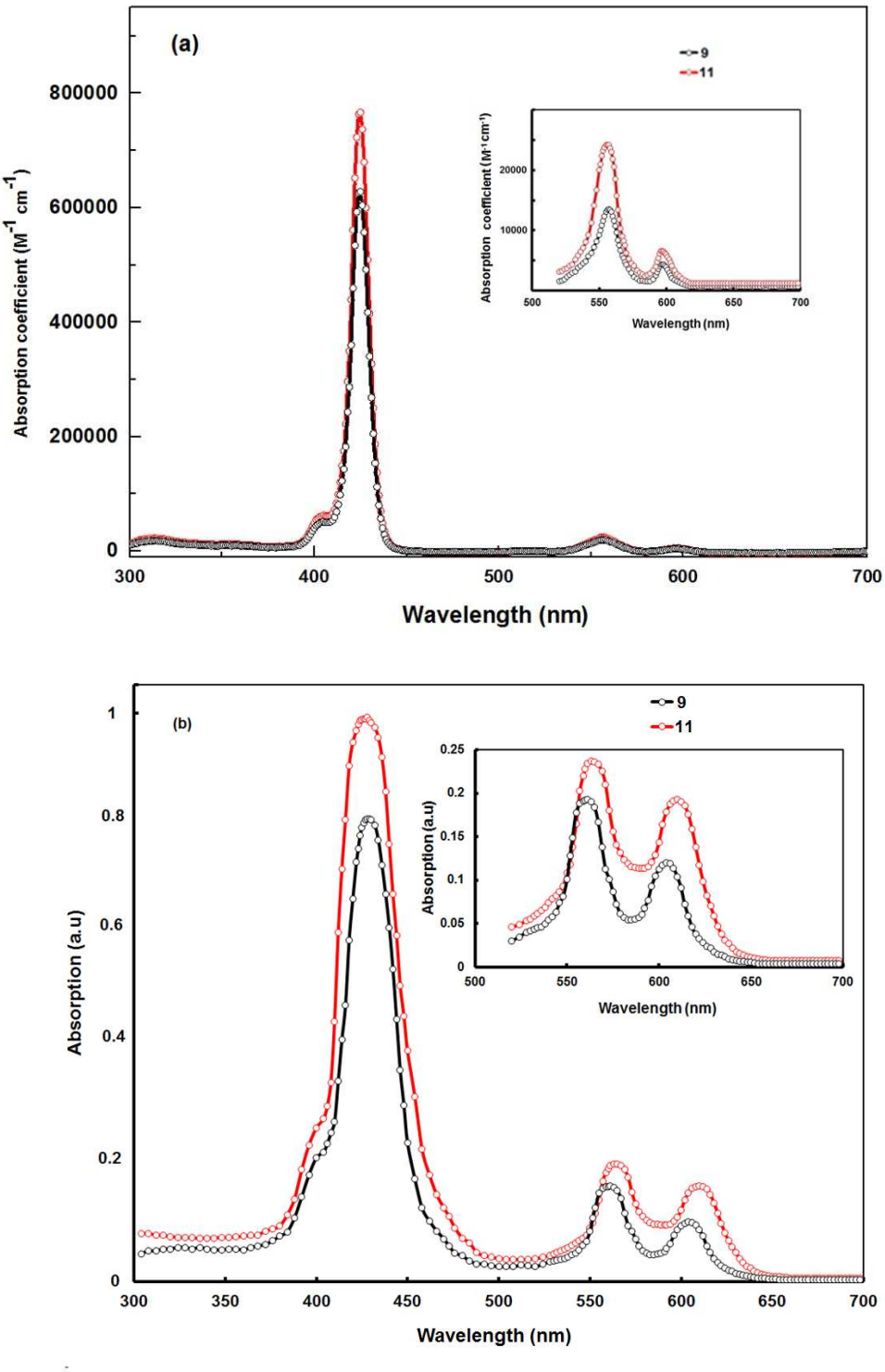

Figure 1. UV-vis absorption spectra of **9** (black color line) and **11** (red color line) (a) in THF solution, and (b) the corresponding spectra when adsorbed onto TiO_2 films.

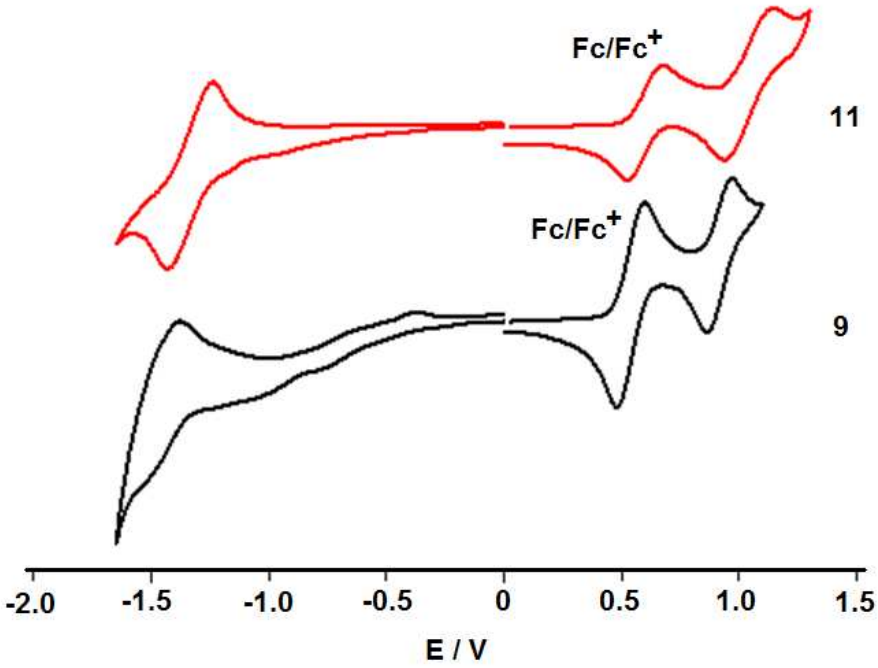

Figure 2. Cyclic voltammograms of **9** (black color line) and **11** (red color line) in THF solutions. The ferrocene/ferrocenium (Fc/Fc^{+}) redox couple wave was observed at 0.55 V *vs* SCE.

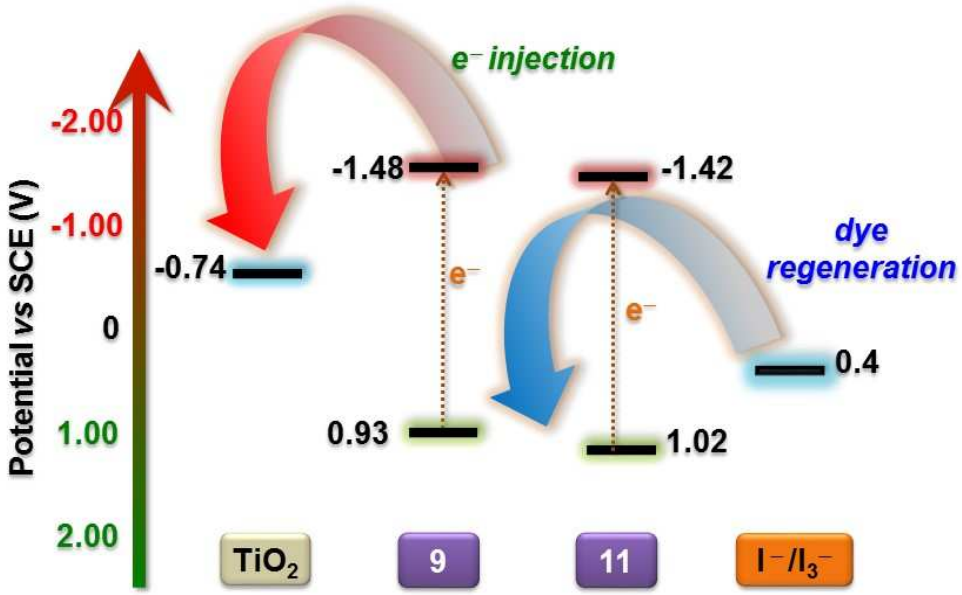

Figure 3. Electrochemical potential diagram showing the electron flow in the **9** and **11** based DSSCs.

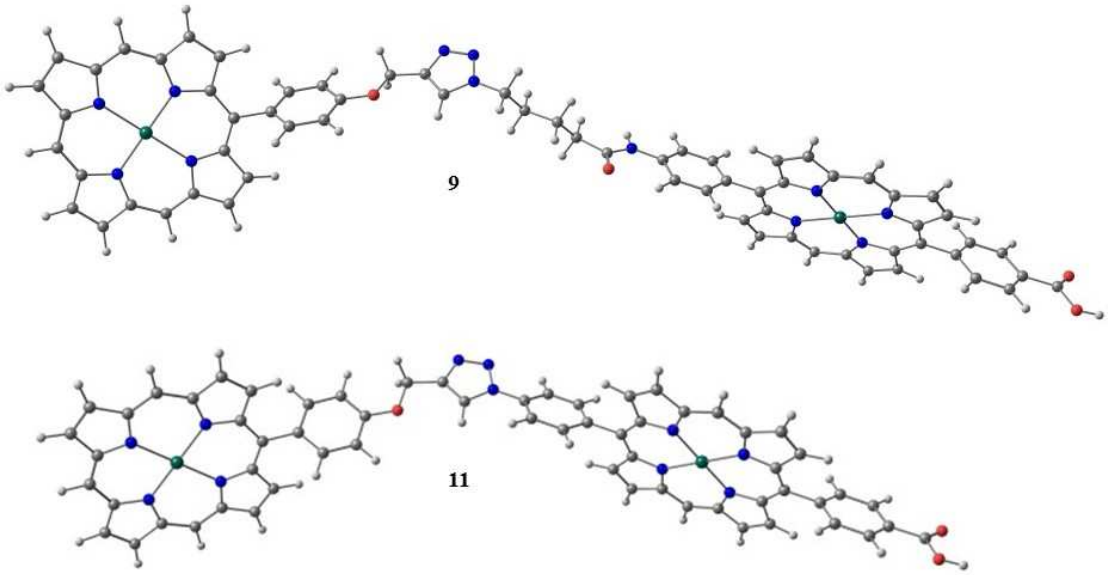

Figure 4. Gas-phase geometry-optimized structure of **9** and **11**. Phenyl and 2,4,6-trimethylphenyl groups are omitted. Carbon, nitrogen, hydrogen, oxygen, and zinc atoms correspond to grey, blue, white, red, and green spheres, respectively.

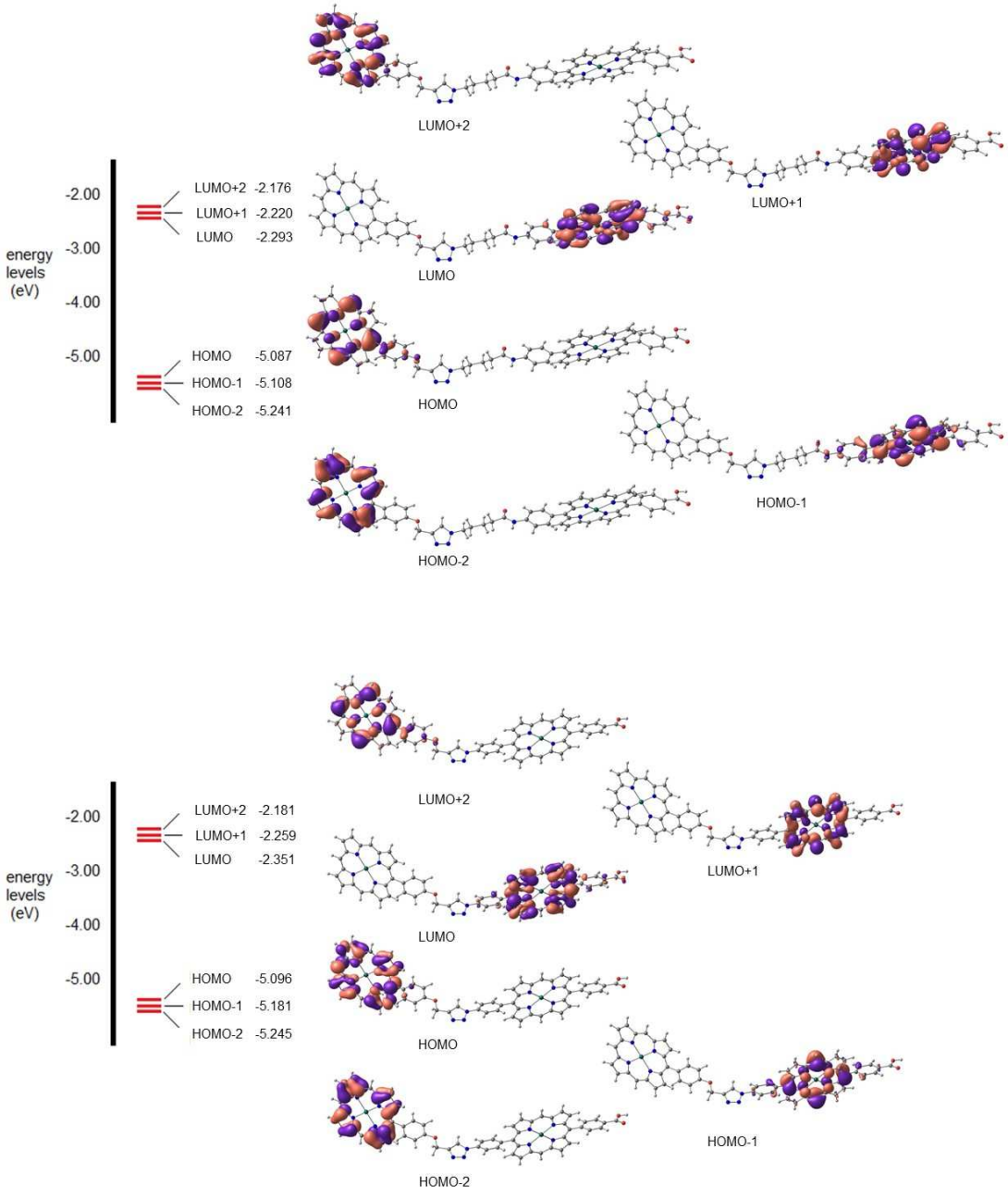

Figure 5. Frontier molecular orbitals and corresponding energy levels of **9** and **11** (upper and lower part of the figure, respectively) from DFT calculation in THF. Phenyl and 2,4,6-trimethylphenyl groups are omitted.

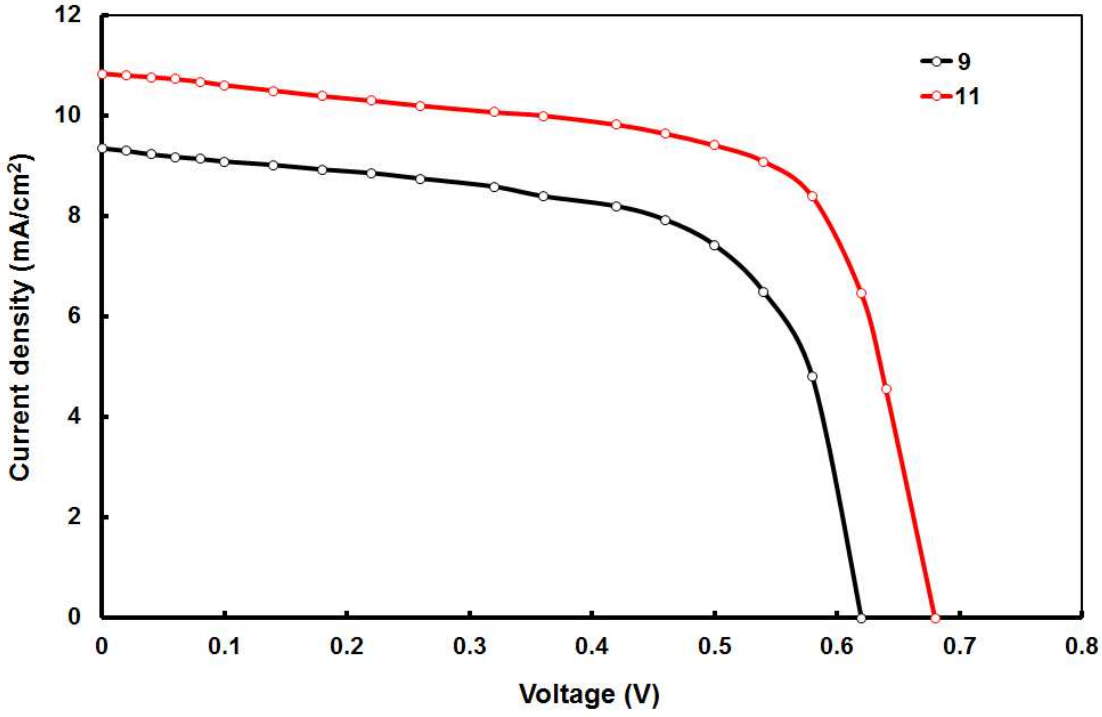

Figure 6. Current-voltage (*J-V*) characteristics of DSSCs based on **9** (black color line) and **11** (black color line), under illumination.

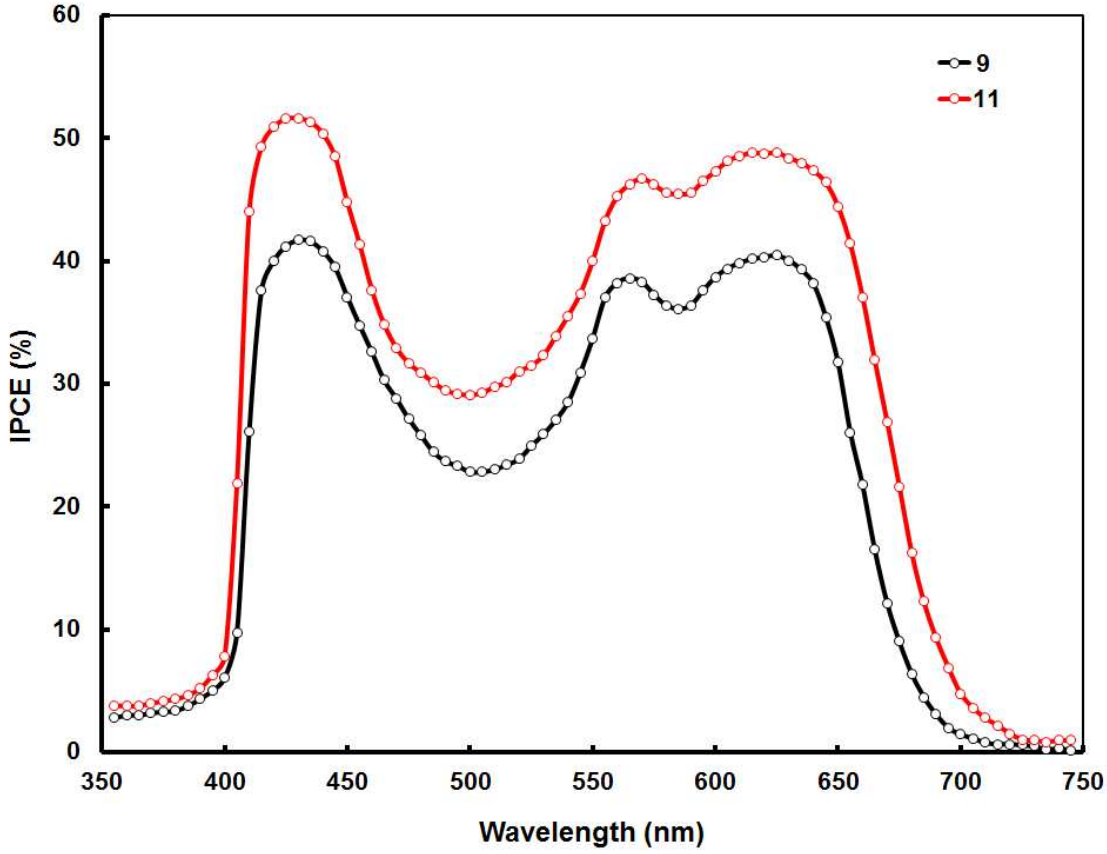

Figure 7. IPCE spectra of DSSCs based on **9** (black color line) and **11** (red color line).

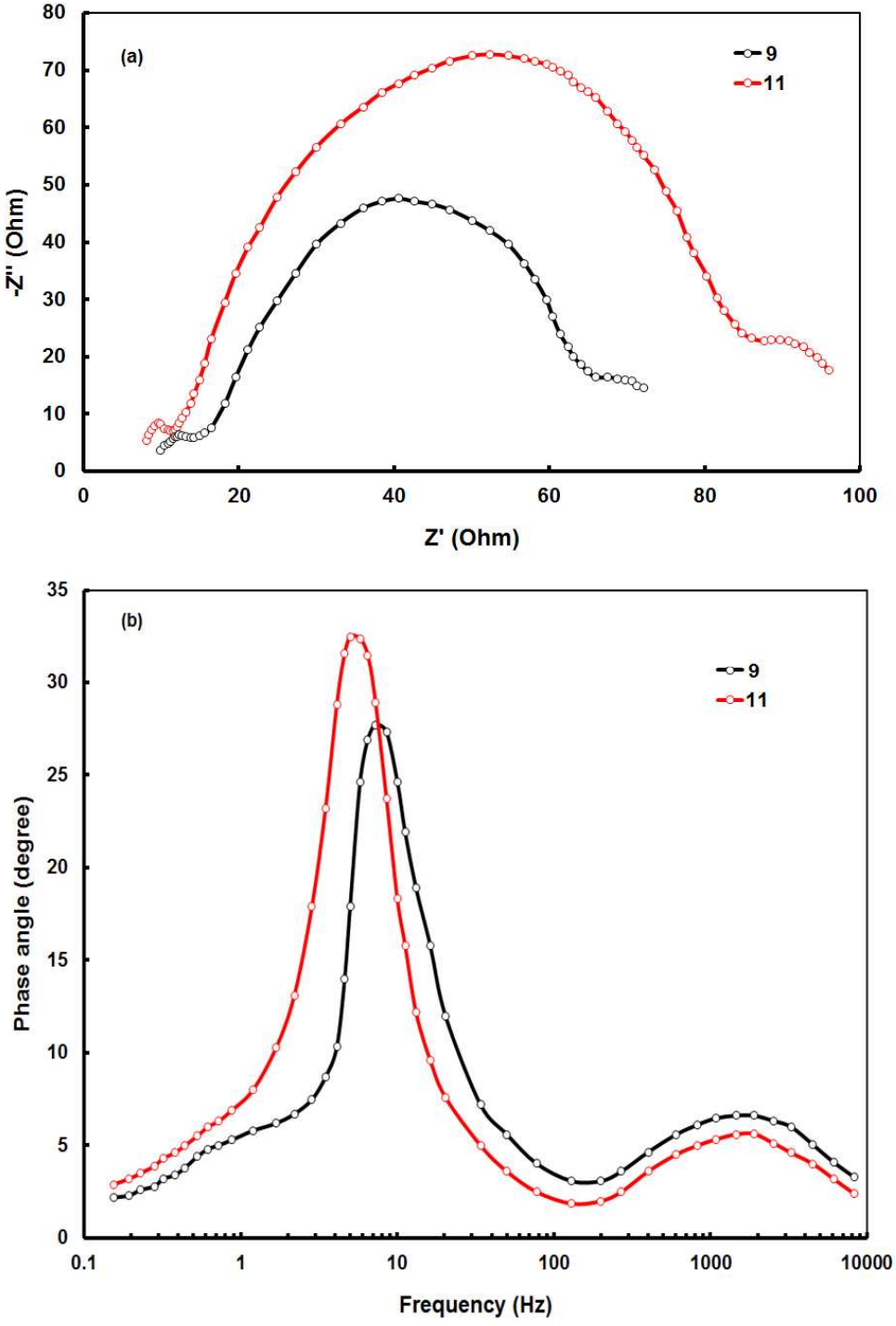

Figure 8. (a) Nyquist plots and (b) Bode phase plots of electrochemical impedance spectra of DSSCs based on **9** and **11** (black and red color lines respectively), measured at a bias voltage of 0.65 V under dark conditions.

1. B. Oregan and M. Gratzel, *Nature*, 1991, **353**, 737-740.
2. M. Gratzel, *J. Photoch. Photobio. A*, 2004, **164**, 3-14.
3. M. Gratzel, *J Photoch Photobio C*, 2003, **4**, 145-153.
4. H. S. Jung and J. K. Lee, *J. Phys. Chem. Lett.*, 2013, **4**, 1682-1693.
5. B. E. Hardin, H. J. Snaith and M. D. McGehee, *Nat. Photonics*, 2012, **6**, 162-169.
6. F. Gao, Y. Wang, J. Zhang, D. Shi, M. Wang, R. Humphry-Baker, P. Wang, S. M. Zakeeruddin and M. Gratzel, *Chem. Commun.*, 2008, 2635-2637.
7. Q. J. Yu, Y. H. Wang, Z. H. Yi, N. N. Zu, J. Zhang, M. Zhang and P. Wang, *ACS Nano*, 2010, **4**, 6032-6038.
8. A. Mishra, M. K. R. Fischer and P. Bäuerle, *Angew. Chem. Int. Ed.*, 2009, **48**, 2474-2499.
9. S. P. Singh, M. S. Roy, K. R. J. Thomas, S. Balaiah, K. Bhanuprakash and G. D. Sharma, *J. Phys. Chem. C*, 2012, **116**, 5941-5950.
10. S. Haid, M. Marszalek, A. Mishra, M. Wielopolski, J. Teuscher, J. E. Moser, R. Humphry-Baker, S. M. Zakeeruddin, M. Gratzel and P. Bauerle, *Adv. Funct. Mater.*, 2012, **22**, 1291-1302.
11. B. G. Kim, K. Chung and J. Kim, *Chem. -Eur. J.*, 2013, **19**, 5220-5230.
12. C. J. Qin, W. Y. Wong and L. Y. Han, *Chem-Asian J*, 2013, **8**, 1706-1719.
13. S. Chang, H. D. Wang, Y. Hua, Q. Li, X. D. Xiao, W. K. Wong, W. Y. Wong, X. J. Zhu and T. Chen, *J. Mater. Chem. A*, 2013, **1**, 11553-11558.
14. Y. Hua, S. Chang, D. D. Huang, X. Zhou, X. J. Zhu, J. Z. Zhao, T. Chen, W. Y. Wong and W. K. Wong, *Chem. Mater.*, 2013, **25**, 2146-2153.
15. D. P. Hagberg, X. Jiang, E. Gabrielsson, M. Linder, T. Marinado, T. Brinck, A. Hagfeldt and L. C. Sun, *J. Mater. Chem.*, 2009, **19**, 7232-7238.
16. W. J. Wu, J. B. Yang, J. L. Hua, J. Tang, L. Zhang, Y. T. Long and H. Tian, *J. Mater. Chem.*, 2010, **20**, 1772-1779.
17. D. Wang, S. C. Hou, H. W. Wu, C. Zhang, Z. Z. Chu and D. C. Zou, *J. Mater. Chem.*, 2011, **21**, 6383-6388.
18. X. Cai, S. C. Hou, H. W. Wu, Z. B. Lv, Y. P. Fu, D. Wang, C. Zhang, H. Kafafy, Z. Z. Chu and D. C. Zou, *Phys. Chem. Chem. Phys.*, 2012, **14**, 125-130.
19. L. L. Li and E. W. G. Diau, *Chem. Soc. Rev.*, 2013, **42**, 291-304.
20. H. M. Zhan, S. Lamare, A. Ng, T. Kenny, H. Guernon, W. K. Chan, A. B. Djurisic, P. D. Harvey and W. Y. Wong, *Macromolecules*, 2011, **44**, 5155-5167.
21. W. K. Wong, X. Zhu and W. Y. Wong, *Coord. Chem. Rev.*, 2007, **251**, 2386-2399.
22. X. J. Zhu, W. K. Wong, W. Y. Wong and X. P. Yang, *Eur. J. Inorg. Chem.*, 2011, 4651-4674.
23. A. Kay and M. Gratzel, *J. Phys. Chem.*, 1993, **97**, 6272-6277.
24. M. K. Nazeeruddin, R. Humphry-Baker, D. L. Officer, W. M. Campbell, A. K. Burrell and M. Gratzel, *Langmuir*, 2004, **20**, 6514-6517.
25. Q. Wang, W. M. Carnpbell, E. E. Bonfantani, K. W. Jolley, D. L. Officer, P. J. Walsh, K. Gordon, R. Humphry-Baker, M. K. Nazeeruddin and M. Gratzel, *J. Phys. Chem. B*, 2005, **109**, 15397-15409.
26. W. M. Campbell, K. W. Jolley, P. Wagner, K. Wagner, P. J. Walsh, K. C. Gordon, L. Schmidt-Mende, M. K. Nazeeruddin, Q. Wang, M. Gratzel and D. L. Officer, *J. Phys. Chem. C*, 2007, **111**, 11760-11762.

27. J. K. Park, J. P. Chen, H. R. Lee, S. W. Park, H. Shinokubo, A. Osuka and D. Kim, *J. Phys. Chem. C*, 2009, **113**, 21956-21963.
28. M. Ishida, S. W. Park, D. Hwang, Y. B. Koo, J. L. Sessler, D. Y. Kim and D. Kim, *J. Phys. Chem. C*, 2011, **115**, 19343-19354.
29. V. S. Y. Lin, S. G. Dimagno and M. J. Therien, *Science*, 1994, **264**, 1105-1111.
30. S. Cherian and C. C. Wamser, *J. Phys. Chem. B*, 2000, **104**, 3624-3629.
31. T. E. O. Screen, K. B. Lawton, G. S. Wilson, N. Dolney, R. Ispasoiu, T. Goodson, S. J. Martin, D. D. C. Bradley and H. L. Anderson, *J. Mater. Chem.*, 2001, **11**, 312-320.
32. J. Rochford, D. Chu, A. Hagfeldt and E. Galoppini, *J. Am. Chem. Soc.*, 2007, **129**, 4655-4665.
33. J. R. Stromberg, A. Marton, H. L. Kee, C. Kirmaier, J. R. Diers, C. Muthiah, M. Taniguchi, J. S. Lindsey, D. F. Bocian, G. J. Meyer and D. Holten, *J. Phys. Chem. C*, 2007, **111**, 15464-15478.
34. S. Eu, S. Hayashi, T. Umeyama, A. Oguro, M. Kawasaki, N. Kadota, Y. Matano and H. Imahori, *J. Phys. Chem. C*, 2007, **111**, 3528-3537.
35. H. P. Lu, C. Y. Tsai, W. N. Yen, C. P. Hsieh, C. W. Lee, C. Y. Yeh and E. W. G. Diau, *J. Phys. Chem. C*, 2009, **113**, 20990-20997.
36. C. P. Hsieh, H. P. Lu, C. L. Chiu, C. W. Lee, S. H. Chuang, C. L. Mai, W. N. Yen, S. J. Hsu, E. W. G. Diau and C. Y. Yeh, *J. Mater. Chem.*, 2010, **20**, 1127-1134.
37. S. L. Wu, H. P. Lu, H. T. Yu, S. H. Chuang, C. L. Chiu, C. W. Lee, E. W. G. Diau and C. Y. Yeh, *Energ. Environ.l Sci.*, 2010, **3**, 949-955.
38. C. W. Lee, H. P. Lu, C. M. Lan, Y. L. Huang, Y. R. Liang, W. N. Yen, Y. C. Liu, Y. S. Lin, E. W. G. Diau and C. Y. Yeh, *Chem-Eur J*, 2009, **15**, 1403-1412.
39. K. K. Pasunooti, J. L. Song, H. Chai, P. Amaladass, W. Q. Deng and X. W. Liu, *J. Photoch. Photobio. A*, 2011, **218**, 219-225.
40. T. Bessho, S. M. Zakeeruddin, C. Y. Yeh, E. W. G. Diau and M. Gratzel, *Angew. Chem. Int. Edit.*, 2010, **49**, 6646-6649.
41. H. P. Lu, C. L. Mai, C. Y. Tsia, S. J. Hsu, C. P. Hsieh, C. L. Chiu, C. Y. Yeh and E. W. G. Diau, *Phys. Chem. Chem. Phys.*, 2009, **11**, 10270-10274.
42. A. Yella, H. W. Lee, H. N. Tsao, C. Y. Yi, A. K. Chandiran, M. K. Nazeeruddin, E. W. G. Diau, C. Y. Yeh, S. M. Zakeeruddin and M. Gratzel, *Science*, 2011, **334**, 629-634.
43. S. Mathew, A. Yella, P. Gao, R. Humphry-Baker, B. F. E. Curchod, N. Ashari-Astani, I. Tavernelli, U. Rothlisberger, M. K. Nazeeruddin and M. Gratzel, *Nature Chemistry*, 2014, **6**, 242-247.
44. P. J. Angiolillo, V. S. Y. Lin, J. M. Vanderkooi and M. J. Therien, *J. Am. Chem. Soc.*, 1995, **117**, 12514-12527.
45. A. J. Mozer, M. J. Griffith, G. Tsekouras, P. Wagner, G. G. Wallace, S. Mori, K. Sunahara, M. Miyashita, J. C. Earles, K. C. Gordon, L. C. Du, R. Katoh, A. Furube and D. L. Officer, *J. Am. Chem. Soc.*, 2009, **131**, 15621-+.
46. J. K. Park, H. R. Lee, J. P. Chen, H. Shinokubo, A. Osuka and D. Kim, *J. Phys. Chem. C*, 2008, **112**, 16691-16699.
47. A. B. F. Martinson, T. W. Hamann, M. J. Pellin and J. T. Hupp, *Chem. -Eur. J.*, 2008, **14**, 4458-4467.
48. A. Tsuda and A. Osuka, *Science*, 2001, **293**, 79-82.
49. Y. Z. Liu, H. Lin, J. T. Dy, K. Tamaki, J. Nakazaki, D. Nakayama, S. Uchida, T. Kubo and H. Segawa, *Chem. Commun.*, 2011, **47**, 4010-4012.
50. G. E. Zervaki, M. S. Roy, M. K. Panda, P. A. Angaridis, E. Chrissos, G. D. Sharma and A. G. Coutsolelos, *Inorg Chem*, 2013, **52**, 9813-9825.

51. G. E. Zervaki, P. A. Angaridis, E. N. Koukaras, G. D. Sharma and A. G. Coutsolelos, *Inotg. Chem. Front.*, 2014, **1**, 256-270.
52. G. E. Zervaki, E. Papastamatakis, P. A. Angaridis, V. Nikolaou, M. Singh, R. Kurchania, T. N. Kitsopoulos, G. D. Sharma and A. G. Coutsolelos, *Eur. J. Inorg. Chem.*, 2014, **2014**, 1020-1033.
53. K. Sonogashira, *J. Organomet. Chem.*, 2002, **653**, 46-49.
54. R. F. Heck and J. P. Nolley, *J. Org. Chem.*, 1972, **37**, 2320-&.
55. A. De Meijere and F. E. Meyer, *Angew. Chem. Int. Edit.*, 1994, **33**, 2379-2411.
56. J. K. Stille, *Angew. Chem. Int. Edit.*, 1986, **25**, 508-523.
57. N. Miyaura and A. Suzuki, *Chem. Rev.*, 1995, **95**, 2457-2483.
58. D. S. Surry and S. L. Buchwald, *Chemical Science*, 2011, **2**, 27-50.
59. J. F. Hartwig, *Pure Appl. Chem.*, 1999, **71**, 1417-1423.
60. H. C. Kolb, M. G. Finn and K. B. Sharpless, *Angew. Chem. Int. Edit.*, 2001, **40**, 2004-+.
61. P. Thirumurugan, D. Matosiuk and K. Jozwiak, *Chem. Rev.*, 2013, **113**, 4905-4979.
62. V. D. Bock, H. Hiemstra and J. H. van Maarseveen, *Eur. J. Org. Chem.*, 2006, 51-68.
63. D. M. Shen, C. Liu and Q. Y. Chen, *Eur. J. Org. Chem.*, 2007, 1419-1422.
64. M. Severac, L. Le Pleux, A. Scarpaci, E. Blart and F. Odobel, *Tetrahedron Lett*, 2007, **48**, 6518-6522.
65. Y. Pareek and M. Ravikanth, *Eur. J. Org. Chem.*, 2011, 5390-5399.
66. V. S. Shetti and M. Ravikanth, *Eur J Org Chem*, 2010, 494-508.
67. Y. Pareek and M. Ravikanth, *Tetrahedron*, 2013, **69**, 7943-7949.
68. E. Ganapathi, S. Madhu and M. Ravikanth, *Tetrahedron*, 2014, **70**, 664-671.
69. Y. Pareek and M. Ravikanth, *RSC Adv.*, 2014, **4**, 7851-7880.
70. M.-E. Ragoussi and T. Torres, *Chem. -Asian. J.*, 2014, **9**, 2676-2707.
71. S. Punidha, J. Sinha, A. Kumar and M. Ravikanth, *J. Org. Chem.*, 2008, **73**, 323-326.
72. K. M. Mikhailov, I. V. Shelaev, F. E. Gostev, Y. P. Yashchuk, V. S. Tyurin, I. P. Beletskaya and V. A. Nadtochenko, *High Energ. Chem.*, 2014, **48**, 276-281.
73. H. Imahori, S. Hayashi, H. Hayashi, A. Oguro, S. Eu, T. Umeyama and Y. Matano, *J Phys Chem C*, 2009, **113**, 18406-18413.
74. Q. L. Tan, X. J. Zhang, L. J. Mao, G. Q. Xin and S. F. Zhang, *J Mol Struct*, 2013, **1035**, 400-406.
75. A. S. Hart, B. K. C. Chandra, H. B. Gobeze, L. R. Sequeira and F. D'Souza, *Acs Appl Mater Inter*, 2013, **5**, 5314-5323.
76. F. L. Wang, J. G. Tang, J. X. Liu, Y. Wang, R. Wang, L. Niu, L. J. Huang and Z. Huang, *J. Phys. Org. Chem.*, 2011, **24**, 1101-1109.
77. W. Kohn and L. J. Sham, *Phys. Rev.*, 1965, **140**, A1133-A1138.
78. R. C. Gaussian 03, Frisch, M. J.; Trucks, G. W.; Schlegel, H. B.; Scuseria, G. E.; Robb, M. A.; Cheeseman, J. R.; Montgomery, Jr., J. A.; Vreven, T.; Kudin, K. N.; Burant, J. C.; Millam, J. M.; Iyengar, S. S.; Tomasi, J.; Barone, V.; Mennucci, B.; Cossi, M.; Scalmani, G.; Rega, N.; Petersson, G. A.; Nakatsuji, H.; Hada, M.; Ehara, M.; Toyota, K.; Fukuda, R.; Hasegawa, J.; Ishida, M.; Nakajima, T.; Honda, Y.; Kitao, O.; Nakai, H.; Klene, M.; Li, X.; Knox, J. E.; Hratchian, H. P.; Cross, J. B.; Bakken, V.; Adamo, C.; Jaramillo, J.; Gomperts, R.; Stratmann, R. E.; Yazyev, O.; Austin, A. J.; Cammi, R.; Pomelli, C.; Ochterski, J. W.; Ayala, P. Y.; Morokuma, K.; Voth, G. A.; Salvador, P.; Dannenberg, J. J.; Zakrzewski, V. G.; Dapprich, S.; Daniels, A. D.; Strain, M. C.; Farkas, O.; Malick, D. K.; Rabuck, A. D.; Raghavachari, K.; Foresman, J. B.; Ortiz, J. V.; Cui, Q.; Baboul, A. G.; Clifford, S.; Cioslowski, J.; Stefanov, B. B.; Liu, G.; Liashenko, A.; Piskorz, P.; Komaromi, I.; Martin, R. L.; Fox, D. J.; Keith, T.; Al-Laham, M. A.; Peng, C. Y.; Nanayakkara, A.;

Challacombe, M.; Gill, P. M. W.; Johnson, B.; Chen, W.; Wong, M. W.; Gonzalez, C.; and Pople, J. A.; Gaussian, Inc., Wallingford CT, 2004.
79. C. T. Lee, W. T. Yang and R. G. Parr, *Phys. Rev. B.*, 1988, **37**, 785-789.
80. A. D. Becke, *Phys. Rev. A*, 1988, **38**, 3098-3100.
81. D. A. Z. Zhurko, G. A. ChemCraft 1.6; Plimus: San Diego, CA. Available at http://www.chemcraftprog.com.
82. V. L. Balke, F. A. Walker and J. T. West, *J. Am. Chem. Soc.*, 1985, **107**, 1226-1233.
83. M. K. Panda, G. D. Sharma, K. R. J. Thomas and A. G. Coutsolelos, *J. Mater. Chem.*, 2012, **22**, 8092-8102.
84. C.-L. Wang, C.-M. Lan, S.-H. Hong, Y.-F. Wang, T.-Y. Pan, C.-W. Chang, H.-H. Kuo, M.-Y. Kuo, E. W.-G. Diau and C.-Y. Lin, *Energ. Environ.l Sci.*, 2012, **5**, 6933-6940.
85. H. Imahori, H. Iijima, H. Hayashi, Y. Toude, T. Umeyama, Y. Matano and S. Ito, *ChemSusChem*, 2011, **4**, 797-805.
86. Y. Wang, X. Li, B. Liu, W. Wu, W. Zhu and Y. Xie, *RSC Adv.*, 2013, **3**, 14780-14790.
87. M. K. Nazeeruddin, A. Kay, I. Rodicio, R. Humphrybaker, E. Muller, P. Liska, N. Vlachopoulos and M. Gratzel, *J. Am. Chem. Soc.*, 1993, **115**, 6382-6390.
88. A. Kira, Y. Matsubara, H. Iijima, T. Umeyama, Y. Matano, S. Ito, M. Niemi, N. V. Tkachenko, H. Lemmetyinen and H. Imahori, *J. Phys. Chem. C*, 2010, **114**, 11293-11304.
89. S. Mathew, H. Iijima, Y. Toude, T. Umeyama, Y. Matano, S. Ito, N. V. Tkachenko, H. Lemmetyinen and H. Imahori, *J. Phys. Chem. C*, 2011, **115**, 14415-14424.
90. J. Bisquert and I. Mora-Seró, *J. Phys. Chem. Lett.*, 2009, **1**, 450-456.
91. F. Fabregat-Santiago, G. Garcia-Belmonte, J. Bisquert, A. Zaban and P. Salvador, *J. Phys. Chem. B*, 2001, **106**, 334-339.
92. A. F. Halverson, K. Zhu, P. T. Erslev, J. Y. Kim, N. R. Neale and A. J. Frank, *Nano Lett.*, 2012, **12**, 2112-2116.
93. Y. D. Lin and T. J. Chow, *J. Mater. Chem.*, 2011, **21**, 14907-14916.
94. S. Q. Fan, C. Kim, B. Fang, K. X. Liao, G. J. Yang, C. J. Li, J. J. Kim and J. Ko, *J. Phys. Chem. C*, 2011, **115**, 7747-7754.
95. Y. P. Hong, J. Y. Liao, D. R. Cao, X. F. Zang, D. B. Kuang, L. Y. Wang, H. Meier and C. Y. Su, *J. Org. Chem.*, 2011, **76**, 8015-8021.